

THESIS FOR THE DEGREE OF DOCTOR OF PHILOSOPHY

Remote Measurements of Gas and Particulate Matter
Emissions from Individual Ships

Jörg Beecken



CHALMERS

Department of Earth and Space Sciences
CHALMERS UNIVERSITY OF TECHNOLOGY
Göteborg, Sweden 2015

Remote Measurements of Gas and Particulate Matter Emissions from Individual Ships
JÖRG BEECKEN
ISBN 978-91-7597-141-4

© JÖRG BEECKEN, 2015.

Doktorsavhandlingar vid Chalmers Tekniska Högskola
Ny serie nr 3822
ISSN 0346-718X

Department of Earth and Space Sciences
Chalmers University of Technology
SE-412 96 Göteborg, Sweden
Telephone + 46 (0) 31 – 772 1000

Cover:
Picture of a ship that was observed during the field campaign in Rotterdam in September 2009 (courtesy of Johan Balzani Lööv).

Typeset by the author using L^AT_EX.

Printed by Chalmers Reproservice
Göteborg, Sweden 2015

to my family

Abstract

Shipping significantly contributes to the world's anthropogenic emissions of sulfur, nitrogen species and particulate matter. These species affect the global radiative forcing as well as local acidification, eutrophication and human health. Studies show that 70 % of the global ship emissions occur within 400 km from land and it is estimated that about 60,000 premature deaths per year are related to these emissions.

The importance of limiting the emission of air pollutants from shipping has been acknowledged by the international community, and policy makers have agreed on international legislation to do this. The current regulations include restrictions for the fuel sulfur content (FSC) and engine specific nitrogen oxide emissions. So far checks of fuel quality are conducted only occasionally, about 200 samples per year in the whole of Sweden, by taking bunker fuel samples as part of on-board inspections of ships at berth in harbors. There is a need for more emission measurements to monitor the compliance of individual ships with respect to the new legislation and to investigate their emissions regarding other pollutants.

In this study, methods are presented which have been developed, as part of the Swedish project Identification of Gross-Polluting Ships (IGPS), to monitor and examine the gas and particulate matter emissions from individual ships remotely using extractive (sniffer) techniques and passive Differential Optical Absorption Spectroscopy (DOAS). Two systems were developed, one fully-automated for the use from ground based stations and a second one for the use on aircraft to analyze ship emissions at open sea. Additionally, a plume capturing method was developed for detailed analysis of the composition of particles in single ship plumes. The mass specific emission factors of SO_2 , NO_x and particulate matter from individual ships were measured from fixed stations, boats, airplanes and helicopters, covering the Baltic and North Sea regions.

Since 2010 the pollutants in ship exhaust of more than 600 individual ship plumes from mobile platforms and more than 3,000 individual plumes from a fixed site at the harbor entrance of Gothenburg were analyzed. The results show a bi-modal behavior for the distribution of the SO_2 emission factors, with international traffic on the higher end around $18 \text{ g}_{\text{SO}_2}/\text{kg}_{\text{fuel}}$ and regional traffic on the lower end around $5 \text{ g}_{\text{SO}_2}/\text{kg}_{\text{fuel}}$. For NO_x , the emissions are distributed around $60 \text{ g}_{\text{NO}_x}/\text{kg}_{\text{fuel}}$. The uncertainties of these emission factors are estimated to be around 20 % and 25 % for SO_2 and NO_x ,

respectively. The majority of the emitted particles are smaller than 100 nm and it was estimated that 70 % of the particle mass is due to particles below 300 nm.

The presented methods can be used for reliable control of compliance to legislation and to provide a level playing field for shipping operators. Conducted measurements indicate a compliance level to the until recently valid 1 % IMO sulfur limit of about 85 % for ships at open-sea and of more than 90 % for ships in or near to harbors. A clear impact of the recently introduced sulfur limit of 0.1 % to the observed SO₂ emissions can be seen.

Keywords: ship emission, pollution, emission factors, particle emissions, compliance monitoring, shipping, identification of polluting ships.

Appended Publications

The following papers reflect the main scientific outcome of my PhD project and are appended to this thesis:

Paper A: J. M. Balzani Lööv, B. Alföldy, L. F. L. Gast, J. Hjorth, F. Lagler, J. Mellqvist, **J. Beecken**, N. Berg, J. Duyzer, H. Westrate, D. P. J. Swart, A. J. C. Berkhout, J.-P. Jalkanen, A. J. Prata, G. R. van der Hoff, and A. Borowiak, "Field test of available methods to measure remotely SO_x and NO_x emissions from ships," *Atmos. Meas. Tech.*, vol. 7, pp. 2597-2613, August 2014

Paper B: **J. Beecken**, J. Mellqvist, K. Salo, J. Ekholm, and J.-P. Jalkanen, "Airborne emission measurements of SO₂, NO_x and particles from individual ships using a sniffer technique," *Atmos. Meas. Tech.*, vol. 7, pp. 1957-1968, July 2014

Paper C: **J. Beecken**, J. Mellqvist, K. Salo, J. Ekholm, J.-P. Jalkanen, L. Johansson, V. Litvinenko, K. Volodin, and D.A. Frank-Kamenetsky, "Emission factors of SO₂, NO_x and particles from ships in Neva Bay from ground-based and helicopter-borne measurements and AIS-based modeling," *Atmos. Chem. Phys. Discuss.*, vol. 14, pp. 25931-25965, October 2014

Paper D: J. Mellqvist, **J. Beecken**, J. Ekholm, and K. Salo, "Remote Compliance Monitoring of Gas Emissions from Shipping to Enforce International Policies," *manuscript in preparation*

Paper E: K. Salo, **J. Beecken**, J. Mellqvist, and J. Ekholm, "Characterisation of particle emissions from individual ships using plume catching by MEGA-chamber," *manuscript in preparation*

Acronyms

AIS	–	Automatic Identification System
AMS	–	Aerosol Mass Spectrometer
ARINC	–	Aeronautical Radio, Incorporated
BC	–	Black Carbon
CCD	–	Charge-Coupled Device
CPC	–	Condensation Particle Counter
CRDS	–	Cavity Ring-Down Spectroscopy
DEHS	–	Di-Ethyl-Hexyl-Sebacate
DMA	–	Differential Mobility Analyzer
DIAL	–	Differential Absorption LIDAR
DOAS	–	Differential Optical Absorption Spectroscopy
EASA	–	European Aviation Safety Agency
EEPS	–	Engine Exhaust Particle Sizer
EF	–	Emission Factor
FSC	–	Fuel Sulfur Content
FMI	–	Finnish Meteorological Institute
FMPS	–	Fast Mobility Particle Sizer
GMD	–	Geometric Mean Diameter
GPS	–	Global Positioning System
IC	–	Ion Chromatography
IGPS	–	Identification of Gross-Polluting Ships
IMO	–	International Maritime Organization
LIDAR	–	Light Detection And Ranging
LNG	–	Liquefied Natural Gas
LPM	–	Liter Per Minute
MARPOL	–	International Convention for the Prevention of Pollution From Ships
MEGA	–	Multiple Exhaust Gas Analyzer
MEPC	–	Marine Environment Protection Committee
NECA	–	NO _x Emission Control Area
NDIR	–	Non Dispersive Infra-Red (spectroscopy)
NOAA	–	National Oceanic and Atmospheric Administration
OM	–	Organic Matter
OPS	–	Optical Particle Sizer

PILS	–	Particle Into Liquid Sampler
PN	–	Particle Number
PM	–	Particle Mass
SECA	–	Sulfur Emission Control Area
SIRENAS	–	Ship Investigation Remotely about NO _x and SO ₂
SMPS	–	Scanning Mobility Particle Sizer
STEAM	–	Ship Traffic Emission Assessment Model
UV	–	Ultraviolet
UVGasCam	–	UV camera imaging system to quantify (ship) emissions

Contents

Abstract	i
Appended Publications	iii
Acronyms	v
Contents	vii
1 Introduction to topic	1
2 Background and Motivation	3
2.1 General on shipping and ship emissions	3
2.2 Formation of sulfur oxides, nitric oxides, and particulate matter	5
2.3 Emission regulations	5
2.4 The IGPS project	6
3 Measurement and model approaches	9
3.1 Measurement approaches	9
3.2 Emission source identification	10
3.3 Modeled ship emissions by STEAM	11
4 Analysis of gas emissions	13
4.1 Calculations	14
4.2 CO ₂ measurement methods	15
4.3 SO ₂ measurement method	19
4.4 NO _x measurement method	19
5 Analysis of particle emissions	21
5.1 Calculations	21
5.2 Particle counting and sizing	22
5.3 Reliability of the EEPS	25
5.4 Analysis of particle composition	27
6 Optical measurements	29
6.1 Theory	29

6.2	Setup	31
6.3	Retrieval	32
7	Aircraft installation	35
7.1	Instrument racks and probe plate	36
7.2	Operation	39
8	Results	41
8.1	Effect of IMO regulation on SO ₂ emissions from ships	41
8.2	Particle emissions and their relation to the sulfur content	43
8.3	Optical analysis of SO ₂ emissions	46
9	Summary of appended papers	49
10	Conclusions	51
11	Outlook	53
12	Acknowledgments	55
	References	57
	Paper A: Field test of available methods to measure remotely SO_x and NO_x emissions from ships	67
	Paper B: Airborne emission measurements of SO₂, NO_x and particles from individual ships using a sniffer technique	87
	Paper C: Emission factors of SO₂, NO_x and particles from ships in Neva Bay from ground-based and helicopter-borne measurements and AIS-based modeling	101
	Paper D: Remote Compliance Monitoring of Gas Emissions from Shipping to Enforce International Policies	131
	Paper E: Characterisation of particle emissions from individual ships using plume catching by MEGA-chamber	159

Chapter 1

Introduction to topic

Shipping is regarded as a rather energy-effective way of global transport concerning the amount of goods and traveled distance. However, due to lower emission quality standards as compared to for example road-vehicles, emissions from ships contribute significantly to the anthropogenic pollution budget. This problem has been recognized and it has been agreed about legislations to reduce primarily the emissions of sulfur, nitrogen oxides and particulate matter. The limitations directly concern the fuel sulfur content (FSC) and the engine dependent emission of nitrogen oxides.

In this thesis, methods are described for the analysis of ship exhausts remotely from ships in traffic using an extractive, sniffer, technique and optical measurements. These methods were used to evaluate the emissions factors, i.e. the amount of an emitted species relative to the amount of consumed fuel, of individual ships in real-time. Such data are needed to check whether ships comply with new policies but also to evaluate the environmental impact of shipping. The emission factors of sulfur dioxide (SO₂) and nitrogen oxides (NO_x) as well as emission factors of particulate matter and its distribution over a size range between 5 nm and 10 μm are presented. A comparatively high number of ships can be monitored in short time by using the presented remote techniques. Additionally, a method for the capturing of individual plumes for extended extractive analyses is shown. The conducted work behind this thesis is an integrated part of the Swedish project IGPS-plus (Identification of Gross-Polluting Ships) [Mellqvist et al., 2014] and has contributed to the development of the measurement systems and the aquirement of data but mostly in testing, data analysis and dissemination of results.

During the course of this project, several studies were conducted to monitor shipping in various operation environments. Measurements in harbor regions were conducted using land-based sites or other boats positioned downwind of the ship to be monitored. The measurements were conducted from ships going at the open-sea, in harbor areas, and in speed reduced water ways.

The stricter regulation significantly increase the the operational costs for shipping. Thus, there is a need for compliance monitoring to guarantee a level playing field. Within this work it is shown how remote emission measurements can be used to effectively monitor the compliance to current legislation. Two systems for real-time remote compliance control were developed for the mobile and permanent use on land-sites, and from aircraft. This allows to monitor ships in inland water ways, harbors and at open-sea. The system recently received a supplemental type certificate for the use on-board a Piper Navajo airplane, stationed in Denmark, which is now ready for permanent compliance monitoring.

Chapter 2

Background and Motivation

2.1 General on shipping and ship emissions

In 2012, ships transported about 9 billion metric tons of goods. This is nearly 80 % of the worldwide merchandise trade volume [UNCTAD, 2012]. The annual growth is around 3 to 4 %. Eyring et al. [2005a] estimated an increase of the number of trading ships from today's nearly 100,000 ships up to around 150,000 ships in 2050. More than 90 % of the civilian ships above 100 gross tons are using diesel-engines. At the moment, systems using alternative fuels are not reaching sufficiently high efficiencies to compete with diesel engines to be competitive. Thus, alongside with the expected increase trading volume and number of ships, an increase of fuel oil consumption to more than 500 million metric tons for 2050 is estimated [Eyring et al., 2005a]. This would be a significant increase compared to 289 million metric tons in 2001 [Eyring et al., 2005b].

Combustion of fossil fuel by its nature causes the formation of carbon dioxide CO_2 and carbon monoxide CO . Michaelowa and Krause [2000] present a comparison of CO_2 emissions of shipping to those of other means of transport. Shipping shows to be the most energy and emission efficient mode of transport. Considering freight transport, the emission of CO_2 from cargo ships and tankers of 7.7 to 31 g_{CO_2} per metric ton and kilometer can exemplary be compared to 133 to 333 g_{CO_2} per metric ton and kilometer from road transport. However, while there are increasingly tighter regulations on the fuel quality and emissions of road vehicles, these do not apply to ships. The fuel crisis in the 1970's caused that crude oils were refined to distillates with enhanced energy efficiency. Lower quality heavy fuel oil started to be a cheap fuel alternative for ship owners with the consequence of increased emissions of pollutants like sulfuric effluents and particles [Corbett and Fischbeck, 1997].

In several studies the global inventory and regional distribution of pollutants has been modeled. Corbett and Fischbeck [1997] used a activity-based model to access the global emission of SO_2 and NO_x emissions due to global shipping. Their model is

based on the engine specific pollutant emission factors, depending on engine specifications and fuel type, the percentage of vessels using the specific engine type as well as the total annual amount of used marine fuel. Based on fuel consumption data from 1993 and world fleet data from 1996, they found that ships contribute to the globally emitted sulfur with 4.24 Tg(S)/year and 3.08 Tg(N)/year, corresponding to 16 % of all sulfur from petroleum use and 14 % of all nitrogen emissions from combustion of fossil fuels. This data is presented spatially resolved in Corbett et al. [1999], showing that nearly 70 % of ship emissions occur close enough for the ship pollutants to reach the shore. Similar activity-based models but with different assumptions have been used in the following studies by Endresen et al. [2003], Corbett and Koehler [2004] and Eyring et al. [2005b]. Endresen et al. [2003] discussed global and local effects to climate and environment based on their emission inventory studies, while the model results of historical evolution of pollutant emission due to shipping is discussed in Endresen et al. [2007] and Eyring et al. [2005b].

A new approach for the modeling of ship emissions has been used by Johansson et al. [2014] finding a reduction of 29 % of SO_x and 17 % of PM_{2.5} emissions from shipping between the years 2009 and 2011 due to change of the allowed FSC. This assessment is based on the Ship Traffic Emission Assessment Model (STEAM) of the Finnish Meteorological Institute [Jalkanen et al., 2009, 2012]. The model uses information about vessel specific emission characteristics and position reports to assess the total emission in the Baltic and North Sea region based on integrated emissions from individual ships.

Different types of measurement studies have been carried out to quantify the emissions of ships. Engine exhaust studies were conducted in laboratories and on-board ships, where the exhaust composition was analyzed at different stages after the combustion process [Moldanova et al., 2009] or for different loads [Winnes and Fridell, 2010, Anderson et al., 2015, Moldanova et al., 2013] and fuel types [Winnes and Fridell, 2009, Moldanova et al., 2013]. Moldanova et al. [2013] and Petzold et al. [2010] found that an increased fraction of the sulfur in the fuel oxidizes to sulphate with increasing engine load.

In other studies the ship exhaust has been analyzed remotely, using land-based sites close to shipping lanes, other vessels or aircraft [Mellqvist et al., 2008, Mellqvist and Berg, 2010] to analyze plume samples downwind of the sources. Diesch et al. [2013] analyzed the chemical composition of plumes from passing ships on the river Elbe from a land-based site. Pirjola et al. [2014] conducted land-based measurements of gaseous and particulate effluents from passing ships in two harbor areas. They could see the effects of different NO_x reducing techniques used on-board vessels, e.g. an increase of particle emissions when direct water injection or humid air motors are used. Schlager et al. [2006] conducted airborne measurements of the enhanced pollutant levels in the English Channel due to shipping. Lack et al. [2009] conducted broad studies of emitted particulate matter from more than 200 vessels measured from a NOAA research vessel. Chen et al. [2005] analyzed the chemistry in a ship plume from airborne measurements outside California and compared it with a photochemical model. They

showed that the lifetime of NO_x was shorter than anticipated. Lack et al. [2011] used airborne measurements to analyze the influence of the reduction of speed and FSC to the plume chemistry finding significantly lower emissions for both, gas species and particles.

2.2 Formation of sulfur oxides, nitric oxides, and particulate matter

Besides carbon dioxide CO_2 , the pollutants sulfur dioxide (SO_2), nitrogen oxides (NO_x) and particulate matter are main pollutants of the exhaust from ships. The sulfur emission is directly connected to the FSC. Moldanova et al. [2009] showed in their study the formation of sulfuric effluents at different stages in the path of the exhaust directly after combustion and after cooling on-board a large cargo vessel during operation. It was seen that most of the sulfur was oxidized to SO_2 and a minor fraction (1 %) to sulfur trioxide (SO_3) which contributes to the formation of sulfuric acid (H_2SO_4).

NO_x , i.e. the sum of NO and NO_2 , is formed mainly from nitrogen in the air due to the high temperatures during combustion. The formation of NO_x increases with the combustion temperature. Ship emission measurements [Alföldy et al., 2013] show that less than 25 % of NO_x is emitted as NO_2 . NO_x is the major component of the emitted NO_y [Chen et al., 2005], i.e. the sum of all nitrogen containing species. NO oxidizes to NO_2 , which in turn is a precursor for nitric acid (HNO_3). Additionally, NO_x is a daytime source of ground-level ozone and contributes to the formation of photochemical smog.

Particulate matter in exhaust from ships consists of organic matter (OM), sulfate (SO_4^{2-}), black carbon (BC) [Lack et al., 2009, Diesch et al., 2013], and ash. Sulfate is directly connected to the FSC [Buhaug et al., 2009]. Diesch et al. [2013] discuss that the emitted OM could be connected to unburned fuel and lubricating oil. The emission of OM was found to depend on FSC, engine type, and load. Black carbon (BC), i.e. strongly light absorbing carbon particles, is formed due to incomplete combustion of fossil fuels.

2.3 Emission regulations

The issues connected to pollutant emissions due to shipping have been recognized worldwide. The International Maritime Organization (IMO) initiated to limit these emissions with the International Convention for the Prevention of Marine Pollution from Ships (MARPOL) Annex VI [MEPC, 2008]. The convention sets limits on the NO_x and SO_x emissions from ships. The European Union adopted the rules in form of directive 2012/33/EU. Because the emissions of SO_x are directly connected to the fuel sulfur content (FSC) according to Buhaug et al. [2009], the IMO limited the maximum

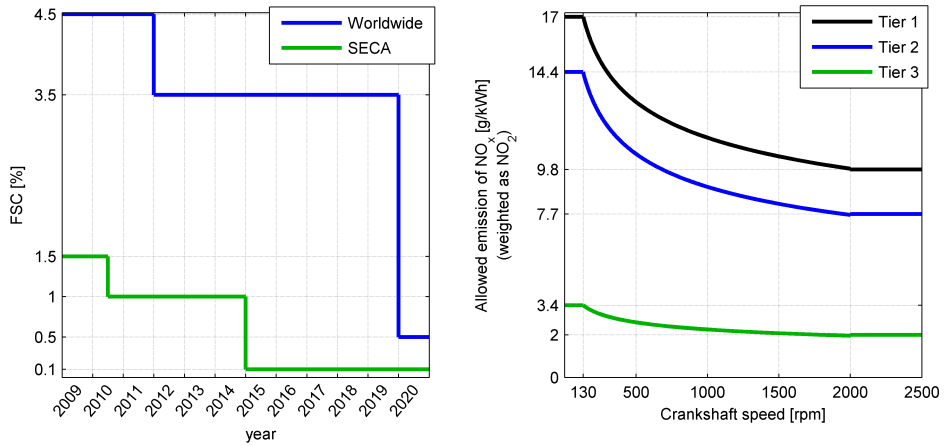


Figure 2.1: MARPOL Annex VI limits for FSC and emission of NO_x from ships.

allowed FSC as shown in Figure 2.1. Furthermore, even stricter limits are introduced in the so called sulfur emission control areas (SECAs). SECAs are currently comprising the entire Baltic Sea, the North Sea, the English channel, and the coastal waters around the USA and Canada.

The regulation of NO_x emission depends on the rated rotational speed of the engine crankshaft, as the formation of NO_x is directly related to combustion temperature in the engine. Slow speed engines are more fuel efficient but produce more NO_x per fuel unit since the combustion temperature is higher. Further, the reduction of nitrogen oxide emission is implemented stepwise. The NO_x emission limits are divided into three tiers. Tier 1 is valid for ships built between 2000 and 2010. Ships that were built after 2010 fall under tier 2. Engines that are installed from 2016 onward have to comply with tier 3. The date of introduction of tier 3 was subject of a recent renegotiation [MEPC, 66th session, April 2014] on which it was eventually agreed to postpone it to January 2021 for northern Europe while it will be implemented around the coast of the US.

2.4 The IGPS project

The large reductions in the sulfur limit for SECAs from 1 % to 0.1 % means a significant increase in fuel costs of about 1,000 Euro per day for a container vessel [Kalli et al., 2009]. Compliance control is needed, to reduce the risk that ships run on non-compliant fuel and to guarantee a level playing field within the shipping sector. Today's methods correspond to the random checks of fuel logs and bunker delivery notes by the port state control. Fuel samples are analyzed occasionally. All these methods are

limited to ships at berth. There is also a need to monitor ships at open sea since the probability of using non-compliant fuel is highest here.

This PhD work contributed to the development of a ground-based and airborne system for remote compliance monitoring of ship pollutants as part of the Swedish project Identification of Gross-Polluting Ships (IGPS-plus) [Mellqvist et al., 2014]. This project is a continuation of a previous one where a prototype system was developed [Berg, 2011, Berg et al., 2012, Mellqvist and Berg, 2010]. The present project encompasses considered two modes of operation: firstly, autonomous compliance monitoring from land-based sites like harbors or close to shipping lanes; secondly, an airborne system for compliance monitoring for ships at open sea.

A stationary system has been in operation since 2012 at the harbor entrance of Gothenburg. It is accessible via the mobile telecommunication network, and plume evaluations for individual, identified ships are retrieved in real-time. A further, airborne system installed on a Navajo Piper airplane, stationed in Denmark, was recently certified (Supplemental Type Certificate 10051623, European Air Safety Agency). It is now ready for permanent use, see Chapter 7.

Chapter 3

Measurement and model approaches

3.1 Measurement approaches

The measurement strategies differ with the platform, i.e. ground-based or airborne measurements.

Ground-based measurements can be carried out in a passive way from the shore or other boats downwind of the shipping lane. The exhaust gas from a passing ship is then transported by the wind towards the observation site. This causes the measurement to be reliant on the wind direction. This is in contrast to measurements from moving platforms by which it is possible to select the ship of interest independent of the wind direction. Two different principles for the measurements from moving platforms are presented here, i.e. extractive measurements, further referred to as sniffer techniques, and optical remote sensing techniques.

The presented ground-based results in this study were mostly obtained from vessels passing fixed measurement stations. Ground-based observations are suitable for measurements close to shore, e.g. in harbors and along ship channels, where the ship traffic is rather dense. Airborne observations, on the other hand, are the means of choice when it comes to monitoring of ship emissions at open sea. The ship traffic is then less dense and yet with the help of aircraft, the emissions of several ships can be analyzed in rather short time.

The sniffer measurements require that the sample is taken inside of the plume, i.e. the inlet has to be located high enough or the aircraft has to fly low enough, respectively, to match the plume height. With sniffer measurements, emission factors, i.e. the mass of emitted pollutant per mass of consumed fuel, can be determined through the ratio of the mixing ratio of the pollutant against the mixing ratio of CO₂.

When applying remote optical measurements, the path integrated concentration of the pollutants SO₂ and NO₂ in the ship plume can be measured from a distance. They can

be retrieved from recorded optical spectra in the UV/visible region using the retrieval principle of Differential Optical Absorption Spectroscopy (DOAS). The emission rates, expressed in mass of the emitted pollutant per unit of time, can be derived by combining the path integrated concentrations with the wind and ship speed. In the scope of this thesis, DOAS measurements using direct or scattered skylight as the light source have been applied upward looking from ground-based platforms and downward looking when used from aircraft. By combining the DOAS measurement of SO_2 with a model calculation of the emitted CO_2 , obtained from STEAM [Jalkanen et al., 2009, 2012], the FSC can be obtained using optical remote sensing techniques. Airborne DOAS measurements can be conducted from higher altitudes, e.g. 300 m, whereas airborne sniffer measurements typically need to be conducted at altitudes between 50 to 100 m.

3.2 Emission source identification

A ship's exhaust plume, that sometimes even can be seen visually, follows the apparent wind which is the superposition of the true ambient wind and the ships motion. This is the wind one feels while being on the deck of a ship. Thus, it is important to know not only the wind direction and speed, but also the ship's navigational data. With this information the apparent wind can be calculated, see Figure 3.1.

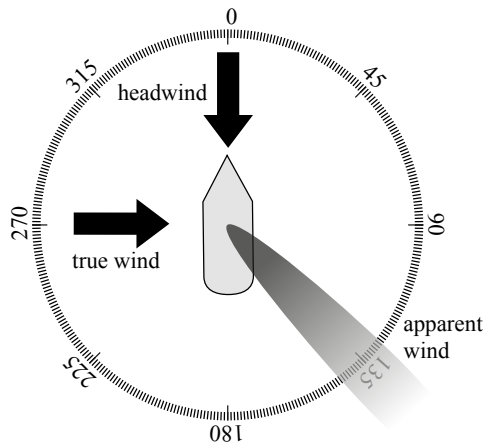


Figure 3.1: Apparent wind: superposition of true wind and the headwind due to the ship's motion, see Berg et al. [2012].

The source of a measured exhaust plume can be identified by calculating the apparent wind speed and direction based on wind measurements and the ships' navigational data that each ship repeatedly transmits as part of the AIS (Automatic Identification System) transponder signal. The transmission of AIS information is compulsory for

ships above 300 gross tons and contains the ship identification number and data about the ship's type, size, position, course and speed, etc.

When measurements are conducted from aircraft, the plumes are crossed in a zigzag-manner starting several kilometers away from the source. Exhaust plumes are usually not visible. Hence, to be able to cross and to analyze it, it is needed to locate the plume quite accurately which is done by calculating the plume position from the apparent wind.

Airborne optical measurements can also be used as an first alert system for compliance monitoring. Airborne studies conducted by Berg et al. [2012] show the feasibility to discriminate between FSCs of 1 % and 0.1 %.

3.3 Modeled ship emissions by STEAM

This study takes into account the modeled emissions from the Ship Traffic Emission Assessment Model (STEAM), developed by the Finnish Meteorological Institute (FMI) [Jalkanen et al., 2009, 2012]. The model calculates the propelling power for individual ships as a function of the ship speed, retrieved from the AIS data. The power consumption here is generally proportional to the cube of the speed. The model accounts for the different engine properties of the ships and the assumed FSC for the calculation of the emission rates for SO_2 , NO_x and various types of particulate matter such as sulfate, organic carbon (OC), elemental carbon (EC) and ash. The model makes use of ship specific data from the IHS Maritime ship register [IHS Global, 2014].

The model provided ship specific data of the break-specific fuel consumption, i.e. the amount of consumed fuel per axial power ($g_{\text{fuel}}/\text{kWh}$), and the mass specific emission factor of NO_x ($g_{\text{NO}_x}/\text{kg}_{\text{fuel}}$). The former was used to convert the measured mass specific emission factors of NO_x to break specific mass emission factors, i.e. mass of NO_x per produced axial power. This value is commonly used, for instance by the IMO to characterize the NO_x emissions since these are strongly dependent on the combustion conditions and hence the engine type, see Figure 2.1. The modeled emission factor of NO_x was also used to correct the measured SO_2 data for NO interference in cases when this value was not measured, see Chapter 4.

A comparison from ground based sniffer measurements of SO_2 , NO_x and particulate matter emission factors to the modeled emissions using the STEAM database is presented in **Paper C**.

Chapter 4

Analysis of gas emissions

This chapter is about the gas analysis of ship plumes using sniffer methods. Such measurements are the backbone of the data obtained within this PhD project. A fast response time of the instruments is very important, when measurements were conducted from aircraft because the time that is available for sampling when a plume is traversed by the aircraft is in the order of one second only. Hence, a major criteria for the selection of the sniffer instrumentation was a short response time, t_{90} , which is the time it takes for the instrument to reach 90 % of the final value at a step change. With the sniffer instruments, the volume mixing ratios of CO_2 , SO_2 and NO_x are measured and then converted to mass specific emission factors for individual ships with uncertainties of about 20 % and 25 % for SO_2 and NO_x emission factors, respectively, see **Paper B** and **Paper C**. The sniffer instruments which were used in this project are presented in Table 4.1 and discussed in the following sections. The shown precisions and accuracies in the mixing ratios for the instruments were retrieved from calibration measurements during a measurement campaign in Kiel in 2011 except for the LI-7000.

Table 4.1: Instrument response time, precision ($1 \cdot \sigma$) obtained from calibrations

Instrument	Gas	t_{90}	$1 \cdot \sigma$
Picarro G2301-m	CO_2	<1 s	< 0.1 ppm
LICOR LI-7000 ^a	CO_2	<0.1 s	< 0.1 ppm
LICOR LI-7200	CO_2	<0.1 s	0.2 ppm
Thermo 43i-TLE	SO_2	2 s	5.1 ppb
Thermo 42i-TL	NO_x	1 s	1.0 ppb

^acalculated from measurements at Gothenburg harbor in 2010

4.1 Calculations

The focus in these studies is on the analysis of the mass specific emission factors, i.e. grams pollutant per kilogram of fuel. In the exhaust plumes, the emitted gases mixes with the ambient atmosphere, effectively superposing onto the background value. Thus the relative quantities of the emitted gases can be retrieved by subtracting the measured mixing ratios of each species in the ship plumes by it's ambient background. An example of the measured mixing ratios and concentrations is shown in Figure 4.1 for an exhaust plume that passes over a fixed measurement site.

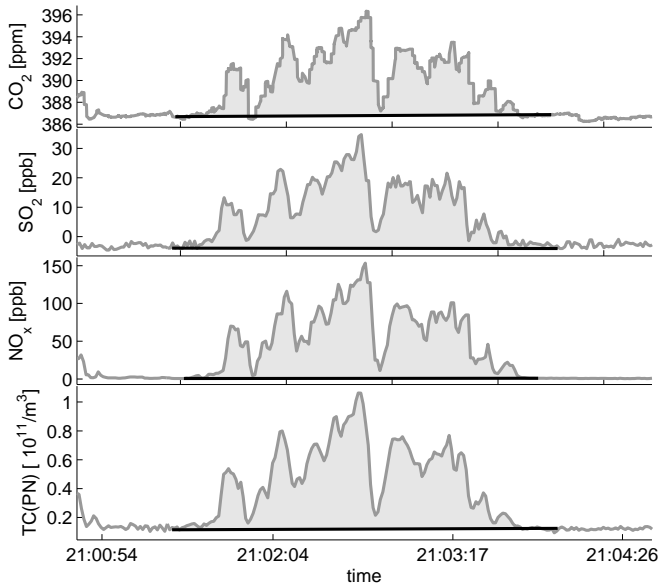


Figure 4.1: A measurement of mixing ratios of CO_2 , SO_2 , NO_x and particle number in the exhaust plume of the RoRo cargo vessel Pauline Russ. The mass specific emission factors are retrieved from these data. The grayish area is the time-integrated mixing ratio or concentration of the pollutant above ambient due to the ship exhaust.

The volume mixing ratios are integrated over the plume after they were subtracted with the respective background values in the ambient atmosphere. CO_2 is a proxy for the carbon in the fuel and used as the reference to which the other quantities are related. For the calculation of the emission factors of other gaseous effluents relative to the amount of combusted fuel, it is assumed that the carbon in the fuel is almost entirely oxidized to CO_2 . This is for instance supported by a study by Moldanova et al. [2009] showing from on-board measurements of a large cargo vessel that less

than 0.5 % of the emitted carbon was emitted in other forms than CO₂. It is also assumed that the carbon content in the fuel is 87 % [MEPC, 2005]. Hence the emission factor of SO₂ can be calculated using the measured volume mixing ratios [SO₂] and [CO₂] by

$$EF(\text{SO}_2)_{\text{gSO}_2/\text{kgfuel}} = \frac{M(\text{SO}_2)_{\text{g/mol}} \cdot \int [\text{SO}_2]_{\text{ppb}} - [\text{SO}_{2,\text{bgd}}]_{\text{ppb}} dt}{M(\text{C})_{\text{g/mol}}/0.87 \cdot \int [\text{CO}_2]_{\text{ppm}} - [\text{CO}_{2,\text{bgd}}]_{\text{ppm}} dt}. \quad (4.1)$$

Here $M(\text{SO}_2)$ is the molecular weight and the brackets, e.g. [SO₂], corresponds to measured mixing ratio and [SO_{2,bgd}] to its background level. Under the assumption that all sulfur is emitted as SO₂ the FSC can be calculated by substituting the molar mass of SO₂ with the atomic mass of S.

$$FSC\% = \frac{M(\text{S})_{\text{g/mol}} \cdot \int [\text{SO}_2]_{\text{ppb}} - [\text{SO}_{2,\text{bgd}}]_{\text{ppb}} dt}{10 \cdot M(\text{C})_{\text{g/mol}}/0.87 \cdot \int [\text{CO}_2]_{\text{ppm}} - [\text{CO}_{2,\text{bgd}}]_{\text{ppm}} dt} \quad (4.2)$$

Thus, the FSC is directly proportional to the emission factor of SO₂, i.e. 20 gSO₂/kgfuel correspond to a sulfur fuel content of 1 %.

Following the IMO technical code MEPC.177(58) [2008] the molecular weight of NO_x is assumed to be that of NO₂ though it is primarily NO that is emitted [Alföldy et al., 2013]. This leads to a worst-case estimation of the NO_x emission. Thus the emission factor of NO_x can be calculated using

$$EF(\text{NO}_x)_{\text{gNO}_x/\text{kgfuel}} = \frac{M(\text{NO}_2)_{\text{g/mol}} \cdot \int [\text{NO}_x]_{\text{ppb}} - [\text{NO}_{x,\text{bgd}}]_{\text{ppb}} dt}{M(\text{C})_{\text{g/mol}}/0.87 \cdot \int [\text{CO}_2]_{\text{ppm}} - [\text{CO}_{2,\text{bgd}}]_{\text{ppm}} dt}. \quad (4.3)$$

4.2 CO₂ measurement methods

The CO₂ measurements conducted in this study rely on two different analysis principles, i.e. non-dispersive infrared (NDIR) and cavity ring-down spectroscopy (CRDS). The NDIR technique is well established and has been widely used for CO₂ measurements [Welles and McDermitt, 2005, Burba et al., 2011], in particular for studying plant uptake of CO₂ etc. The CRDS technique has emerged recently, as a state of the art technique for accurate gas concentration measurements of CO₂ [O’Keefe and Deacon, 1988]. Both, NDIR and CRDS utilize the absorption of energy by CO₂ at specific wavelengths in the infrared spectral region. The details of systems and their underlying analysis methods are presented in the following.

In the case of **non-dispersive infrared spectroscopy (NDIR)**, the integrated radiation over a certain spectral band is analyzed. The spectral region of interest, in this case around 4.26 μm, is limited by an optical bandpass filter, which is transparent

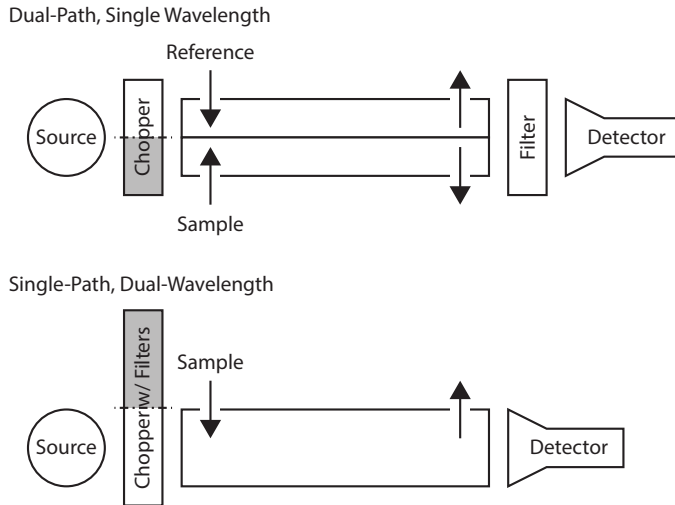


Figure 4.2: Principle of different NDIR setups (adapted from Welles and McDermitt [2005]). The upper scheme correspond to the LI-7000, while the lower one corresponds to the LI-7200.

only in this wavelength region. A heated element which emits broadband radiation in the infrared spectral region is used as light source at one end of a sample cell of known volume and length. The CO₂ contained in the sample air absorbs parts of the incoming radiation along the path of light depending on its concentration, pressure and temperature according to the Beer-Lambert law. A fast solid state detector measures the transmitted radiation at the other end of the sample cell which requires fast chopping of the incoming radiation to work optimally. With the LI-7000 and LI-7200 (both manufactured by LI-COR) two different NDIR instruments have been used. The LI-7000 is designed following a dual-path, single-wavelength scheme, where one path is used as a reference channel surged with air at a known CO₂ concentration, see upper setup in Figure 4.2. There is a small cross-sensitivity to water as it also absorbs in the filter region, which needs to be considered. The LI-7200 on the other hand, is designed in a single-path, multi-wavelength configuration for the analysis of CO₂ and H₂O, using only one cell for the sample gas. Several optical filters are comprised on the chopper wheel to measure the transmitted light in a spectral reference region with no absorption by the key species and specific regions where CO₂ and H₂O absorb. The working principles of the two instruments are shown in Figure 4.2.

The Picarro G2301-m is adapted for flight measurements of CO₂, CH₄, and H₂O based on **cavity ring-down spectroscopy (CRDS)**. In this technique the wavelength of a pulsed laser is tuned across an absorption line of the species to be measured. As shown in Figure 4.3, the laser beam of a certain wavelength enters a resonator filled with the

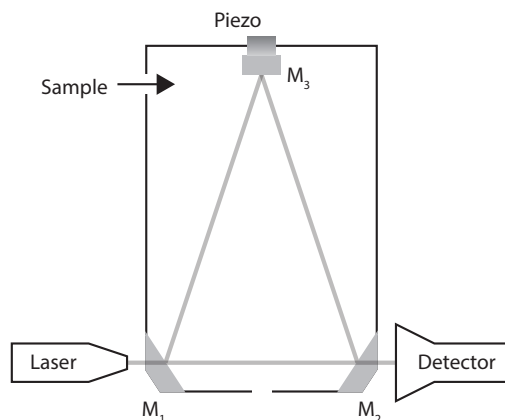


Figure 4.3: Principle of the CRDS (G2301-m) setup. The position of one of the mirrors, M_3 , is adjusted to obtain positive light interference for each wavelength, at the superposition of each round-trip between the mirrors M_1 , M_2 and M_3 .

gas sample. After the laser is turned off, the light continues its round-trip within the resonator. Due to the minimal transmittance of the mirrors a small fraction light intensity can be detected outside the resonator. During its round-trip the intensity of the light is reduced by the mirror losses but also by molecular absorption due contained gas sample. Thus the intensity of light within the resonator is exponentially decreasing over time and as such is also the fraction that is reaching the detector. This decrease is called ring-down, which is the faster the higher the concentration of the absorbing species within the resonator is. In contrast to other techniques like NDIR, where the absorption is measured directly as an absolute ratio of intensities, the absorption in CRDS is related to the time constant of the exponential decay. The decay is increasingly slower for the smaller the concentration of the absorbent species is, making it an ideal method for measuring weak absorption features of trace gas molecules. The laser of the G2301-m is sequentially tuned over the wavelength interval around the specific spectral line. In the G2301-m, the same procedure is repeated in a sequence for the different species at specific wavelength regions and it takes about 1 s for the analyzer to toggle through one sequence for measuring all three species. Since the absolute absorption is measured the need for correction of the baseline drift is eliminated and hence the need for zero air, in contrast to the NDIR instruments.

The flight adapted CRDS analyzer incorporates pressure control of the inlet gas and a pressure correction of the laser wavelength tuning. In addition a tailor-made measurement scheme was implemented. As the focus is on fast and reliable CO_2 measurements, the software of the instrument was custom changed by the supplier adding the option to replace the time slot for CH_4 for one additional CO_2 measurement, such measur-

ing CO₂ about twice per second. The H₂O measurements are kept to correct for the cross-sensitivity of the CO₂ measurements to water [Chen et al., 2010]. Further, the instrument can optionally be switched into a high-flow mode, to enhance the response time of the CO₂ analyzer to less than 1 s. Toxic material, i.e. PVC, was also exchanged in this instrument, as to required to avoid PVC in the instrumentation for the sake of its flight certification.

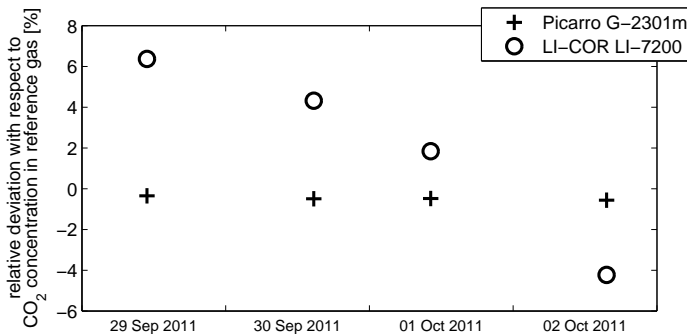


Figure 4.4: Comparison of Picarro G2301-m and LICOR LI-7200 over several calibration periods during the measurement campaign in Kiel in 2011 with respect to their response to reference gases containing 375 ppm and 410 ppm CO₂. While no significant drift could be seen for the the G2301-m, the LI-7200 drifts in average with -3.3 % per day.

The experience from the measurements in this project, and in other studies [Chen et al., 2010] is that the G2301-m is quite reliable and stable over time. Its drift over time compared to the LI-7200 is shown in Figure 4.4. It can be seen that the G2301-m doesn't show any significant drift over the time of the measurement, while LI-7200 drifts with about -3.3 % per day in average. Thus, frequent calibrations are necessary for the latter. However, both the Picarro and the LICOR CO₂ analyzers show similar precisions, as can be seen in Table 4.1. The LI-7200 works without the need of continuous reference gas purging which simplifies it's handling as compared to the LI-7000 model. The two LI-COR models are very compact and both designs are less complex than the G2301-m, which is difficult and combine with other sensors in a compact, common frame. This is in favor for the LI-7200 which was disintegrated and combined with a modified Thermo 43i-TLE SO₂ analyzer for compact, integrated design of a complete compliance monitoring system, as described in Chapter 7. Certainly, the strength of the G2301-m is its stability, but occasionally sampling appears fail which was observed in conjunction with sudden changes. Presumably, the mixing ratio in the resonator changed too sudden and too significant while the laser was tuned over the wavelength interval of the spectral line of interest so that the spectral feature could not be retrieved and analyzed properly.

When this PhD project started, the LI-COR LI-7000 was used as CO₂ analyzer in the IGPS system at that time [Mellqvist and Berg, 2010]. It contained a reference cell, which was continuously surged with reference air with a specific CO₂ concentration. During the course of the project a CRDS based modified Picarro G2301-m was purchased. Due to its precision and ease of use it replaced the LI-COR instrument on some campaigns. But with respect to fast measurements and bearing the form factor of a possibly small measurement box in mind, it was later decided to extend the CO₂ analyzers by a further NDIR analyzer. It was decided to use the LI-7200 because of its benefit of not having the need for continuous surging of the reference cell.

4.3 SO₂ measurement method

The Thermo 43i-TLE trace gas monitor is used for measurements of the SO₂ volume mixing ratio in the plumes. It is based on **UV fluorescence**, where the SO₂ molecules are brought into an short-lived excited state by absorption of energetic radiation in the UV region [Luke, 1997] ($\lambda_1 \approx 190 \dots 230$ nm). The molecule releases the excess energy to fall back into the ground state in form of a photon ($\lambda_2 \approx 200 \dots 400$ nm), which is then measured by a detector. The amount of emitted photons from the fluorescence is proportional to the number of SO₂ molecules, i.e. to its volume mixing ratio given a certain volume and pressure.



The instrument shows cross sensitivity to aromatic volatile organic compounds (VOCs), and NO. For this reason the standard version of the Thermo 43i-TLE contains a hydrocarbon kicker. However, in the case of ship emissions aromatic VOCs are not significant and can be neglected Williams et al. [2009]. Experiments that we carried out to quantify the influence of NO showed that the apparent SO₂ reading corresponds to 1.5 % of the volume mixing ratio of NO, which was corrected at the later data analysis stage. In this project, the applied model of the Thermo 43i-TLE has been custom modified for faster sampling, by removing the flow meter and the hydrocarbon kicker for increasing the flow rate to 6 LPM. The t_{90} response time is 2 s and the sample rate 1 Hz.

4.4 NO_x measurement method

Chemiluminescence is a well established technique for the monitoring of NO_x, i.e. the sum of NO and NO₂, in the environment [Demerjian, 2000, EN 14211, 2012]. The applied Thermo 42i-TL makes use of this method, which makes use of the chemiluminescent reaction with O₃ to measure NO [Kley and McFarland, 1980, Kleffmann et al., 2013].



Reaction (R 4.4) is the desired luminescent reaction ($\lambda \approx 590 \dots 2800 \text{ nm}$) used to detect NO. However, collision with other molecules can lead to quenching (Reaction (R 4.5)), a return into the ground state without the emission of light. The reduction of pressure effectively reduces the probability for quenching. The intensity of the emitted light is proportional to the number of NO molecules, as confirmed by linearity tests during our calibrations of the Thermo 42i-TL.

In order to measure NO_x by chemiluminescence NO₂ must first be reduced to NO. In the Thermo 42i-TL trace gas monitor this is done by a heated molybdenum converter.



The volume mixing ratio of NO₂ can be retrieved from differential measurements. During the course of the IGPS measurements, the Thermo 42i-TL was run in NO_x mode. In this project the chemiluminescence instrument is operated at lower pressure than normal, i.e. 250 mbar instead of 325 mbar, using a stronger pump. This was done to increase the response time and sensitivity. The sample flow is 1 LPM and the instrument provides t_{90} response time of less than 1 s at a sampling rate of 1 Hz.

Chapter 5

Analysis of particle emissions

Ships are large sources for particles composed of ash, soot, organic material and sulfate. It has been shown in several studies that a fraction of the emitted sulfur is found in form of sulfate [Petzold et al., 2008, Moldanova et al., 2009, Murphy et al., 2009, Petzold et al., 2010, Lack et al., 2011, Diesch et al., 2013, Alföldy et al., 2013]. Due to this, there is an extra uncertainty when the fuel sulfur content is determined from the gas phase measurements, which results in a negative bias in the estimated sulfur content. During this work, measurements were conducted in order to quantify the particles that are emitted from ships and to see if there is a direct connection to the fuel sulfur content.

It is more complex to carry out measurements of particulate matter than gases. Particles can be characterized by both, physical and chemical characteristics, which are described in detail by Hinds [1999] and Finlayson-Pitts and Pitts [2000]. They can differ in their physical quantities like size, weight, and optical refraction and chemical characteristics like composition and solubility on the other hand.

5.1 Calculations

The calculation of emission factors for particulate matter is slightly different as for the case of gases as described in Chapter 4 since the absolute concentration is measured, i.e. number or mass of particles per cm^3 , instead of volume mixing ratios. The emission factor of number of particles, $EF(PN)$, can thus be calculated by

$$EF(PN)_{\text{part./kg}_{\text{fuel}}} = \frac{\int [N_{\text{tot}}]_{\text{part./cm}^3} - [N_{\text{tot,bgd}}]_{\text{part./cm}^3} dt}{\int [\text{CO}_2]_{\text{kg/cm}^3} - [\text{CO}_{2,\text{bgd}}]_{\text{kg/cm}^3} dt} \cdot \frac{M(\text{CO}_2)_{\text{g/mol}}}{M(\text{C})_{\text{g/mol}}/0.87}. \quad (5.1)$$

The latter term in Eq. (5.1) is the emission factor of CO_2 which yields $3.19 \text{ kg}_{\text{CO}_2}/\text{kg}_{\text{fuel}}$, assuming that 87 % of the carbon in the fuel is emitted as CO_2 [MEPC, 2005]. The temperature T , pressure p , and the gas constant R are used for the conversion

$$[\text{CO}_2]_{\text{kg/cm}^3} = [\text{CO}_2]_{\text{ppm}} \cdot M(\text{CO}_2)_{\text{g/mol}} \cdot \frac{pPa}{R_{J/(\text{mol}\cdot\text{K})}T_K} \cdot 10^{-15}. \quad (5.2)$$

For the calculations in these studies T and p were assumed to be 290 K and 101325 Pa, respectively. The variable deviations from these values contribute to the uncertainty of the emission factor. This contribution is estimated to be in the order of 5 %.

The particle mass is derived from the individual size distributions of the particulate matter in the emission plumes. The particles are assumed to be spherical in shape and have unit density throughout the entire size range, i.e. 1 g/cm³. Hence, the respective volume can be calculated for each size bin and multiplied by the density to gain a conversion table from particle number to particle mass and integrated to yield the total mass over all size bins, M_{tot} . The emission factor of the particle mass, $EF(PM)$, for individual plumes is calculated analogue to Eq. (5.1) by substituting N_{tot} with M_{tot} .

5.2 Particle counting and sizing

The counting of particles is conducted in various ways. The aim is to count the total number of particles, but also to examine the size distribution of the particles. Important characteristics for the particle instruments are response time and covered size interval. Lyyräinen et al. [2002] reported that most particles can be found in the size range between 40 and 100 nm. The instruments that were used in this PhD study and the taken considerations are presented below.

The **condensation particle counter (CPC)** is a reliable instrument for measuring the total concentration of particles in the specific size range of the counter. The sampled air that contains the particles is guided through a volume which is supersaturated with alcohol or water vapor. The particles act as seeds onto which the vapor condensates and even particles as small as a few nanometers will reach a size that can be detected optically. CPCs have a high comparatively high counting efficiency are stable and seldom need to be calibrated.

Standard CPCs use isopropanol and butanol as condensation liquids. Isopropanol is not recommended for long term use when a large liquid reservoir is needed. Over time water could diffuse into the isopropanol and would interfere with the functionality of the alcohol based CPCs. Using butanol instead, the diffusion of water is much less of a problem, making it more suitable for autonomous operations over longer periods. However, considering the flammability of the alcohols and the subsequent safety issues on-board aircraft, it was decided to use a water-based CPC (TSI 3787) in which distilled water is used as condensing liquid [Hering et al., 2005]. This CPC samples particles in the range from 5 nm to 10 μm and retrieve particle concentrations with an accuracy of about 10 %, as specified by the manufacturer. Its response time, t_{90} ,

is less than 0.3 s.

In an **differential mobility analyzer (DMA)** particles are separated by their size using the size-related electro-mobility. Generally, a DMA consists of a concentric pair of electrodes with a controlled negative voltage on the inner electrode [Intra and Tippayawong, 2008]. Two laminar streams of air are introduced into the annular space between the electrodes, with one containing the previously electrically charged particles of the sample aerosol. This stream is separated from the inner-electrode by a stream of particle-free sheath air. The electrical field perpendicular to the particle stream causes the positively charged particles to be deflected towards the negatively charged, inner electrode along their flow. Particles of higher electro-mobility reach this electrode at an earlier stage than particles of lower electro-mobility, further depending on the streams' flow rates and the geometry of the DMA. Mono-disperse particles, which have a specific electro-mobility, exit the DMA separately from particles with other electro-mobilities through a slit at certain position along the center electrode.

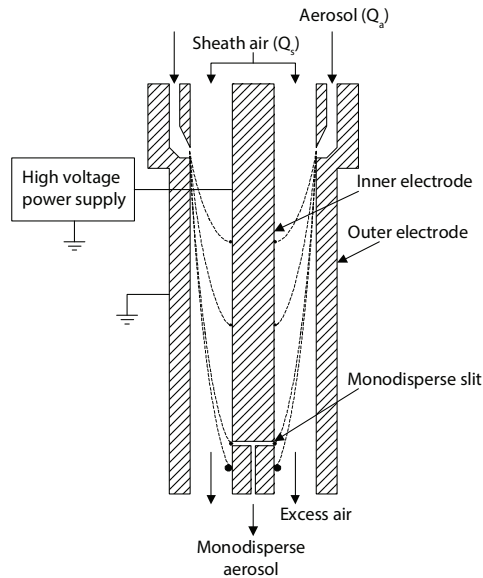


Figure 5.1: Basic principle of a general DMA (adapted from Intra and Tippayawong [2008]).

In an **scanning mobility particle sizer (SMPS)** a DMA is combined with a CPC, to obtain the distribution of the concentration of particles as a function of particle size. This is a standard method also used for defining particles used as reference particles for the validation of size distributions measured by other systems.

The charging of the particles is critical and usually a bipolar diffusion charger [Liu and Pui, 1974] is used to obtain a rather well known charge distribution on the particles [Fuchs, 1963, Wiedensohler, 1988]. In this study the used TSI DMA 3081 covers a size total range from 10 nm up to 1 μm . In the SMPS the size distribution is not measured over all sizes simultaneously, since the voltage is gradually changed. The scanning over a certain size range is therefore a function of time, depending on the width of the size range, accuracy, and response time of the CPC. The scan time typically lies between 10 s up to some hundreds of seconds and this system can only be used for remote measurements of exhaust emissions if the plume is captured and prevailed like described in **Paper E**. The quality of the SMPS was validated in measurements of polystyrene latex spheres of known sizes, and it was observed the system underestimated the size by 1 % with an offset of 7 nm, see **Paper C**.

For fast sampling of particle size distributions, the TSI 3090 **engine exhaust particle sizer (EEPS)** is used. Like the SMPS, the EEPS makes use of the electro-mobility of particles. But in contrast to the DMA, the particles in the EEPS are charged by two consecutive unipolar diffusion chargers of opposite polarity. Firstly, a precharger neutralizes large positive initial charges on the particles, by emission of negatively charged ions from a corona needle. Secondly, positive ions from a stronger charger diffuses onto the particles. The sample stream containing the particles flows along a positively charged electrode in the center of the column, repelling the positively-charged particles away from the center rod towards 22 ring shaped electrometers, mounted atop of each other at the wall of the column. Analogue to the DMA, particles with higher electro-mobilities reach the wall at an earlier stage as compared to those having a lower electro-mobility [Johnson et al., 2004]. When the charged particles impact on the outer electrodes, they cause a current that is measured and which is used to retrieve a particle size distribution between 5.6 and 560 nm in 32 bins instantaneously. The EEPS has a sampling rate of 10 Hz, and response time, t_{90} , of 0.5 s.

Size distributions for particles with diameters above those covered by the EEPS, are analyzed by the **optical particle sizer (OPS)** TSI 3330. This instrument covers the size range from 300 nm to 10 μm in 16 size channels. Single particles in this range are big enough to be detected and characterized optically by the intensity of the backscattered light of a laser pulse onto a flow of sample air. In contrast to the sizing methods mentioned above, this method does not depend on the electro-mobility. Instead, the particle size is related to the intensity of the back scattered light. Thus, there is a dependence on the refractive index and the shape of the individual particle. For the measurements we assumed a real refractive index of 1.59 and a shape correction factor of 1 which corresponds to the properties of polystyrene spheres. During flight, the OPS showed to be very sensitive to changes in pressure and hence requires well controlled flow.

5.3 Reliability of the EEPS

The reliability of the EEPS is currently a subject of discussion. I decided to reflect this discussion at this stage because the EEPS is the main instrument concerning the particle measurements conducted during my PhD studies.

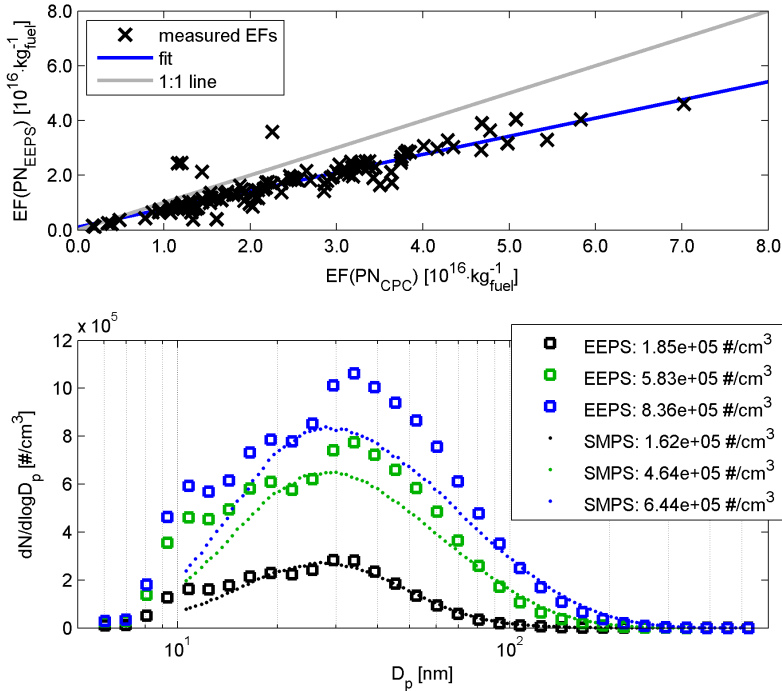


Figure 5.2: Validation of the EEPS. Upper figure: correlation between EEPS and CPC for the cross-validation of total particle count. Lower Figure: comparison between EEPS and SMPS response to ammonium sulfate for the cross-validation of size distribution for different total concentrations (as given in legend).

In studies by Asbach et al. [2009], Jeong and Evans [2009], Kaminski et al. [2013], and Zimmerman et al. [2015] the EEPS, or the similar FMPS (TSI 3091), was compared to SMPS systems and significant differences were found for total concentration and size distribution.

Jeong and Evans [2009] found that the the differences could partly be explained with diffusion losses of particles in the applied SMPS. But they also hypothesized that the differences are also due to the data inversion algorithm of the EEPS. The EEPS

physically measures the distribution of small currents which are produced when the charged particles set on the one of the electrodes. There are 22 physical electrodes, yet the distribution is mathematically treated to represent the size distribution in 32 size bins over the entire size range using an instrument specific inversion scheme. This inversion scheme takes into account multiple charges, voltages over the center electrode, time delays between the electrometers, induced charges, and noise and bias contributions by the electrometers.

Asbach et al. [2009] speculated from their comparison results that different particle morphologies cause differences in particle charging. In contrast to the unipolar charging in the EEPS, particles in the SMPS are charged using bipolar charging. They pointed out that the particle morphology can have a significantly different impact on unipolar and bipolar particle charging. They claimed that the correction suggested by Jeong and Evans [2009] did not work for their measurements.

Kaminski et al. [2013] conducted an extensive comparison of mobility particle sizers in which they also tested three FMPS systems against a calibrated SMPS for NaCl, Di-Ethyl-Hexyl-Sebacate (DEHS), and soot particles, i.e. particles of different size and morphologies. They found that the discrepancy considering particle sizing was about $\pm 25\%$ and the discrepancy considering the total concentration was about $\pm 30\%$, as compared to CPC and SMPS results, respectively. Their comparison also showed that FMPS accuracy depends on both, particle size and morphology. They assumed that this is due to different shape dependent charging probabilities between bipolar charging, as in the SMPS, and unipolar charging, as used in the FMPS and EEPS.

There appears to be possibly residual peak in the particle distributions around 10 nm [Asbach et al., 2009, Jeong and Evans, 2009, Kaminski et al., 2013], for which to my knowledge no explanation was found, yet. However, Zimmerman et al. [2015] developed a extended correction procedure based on their own comparison studies and the suggestions of Jeong and Evans [2009].

To validate the performance of the EEPS used in our studies it was compared against the CPC and the SMPS. A good correlation ($R^2=0.83$) of the EEPS with the CPC can be seen in a comparison of the results from simultaneously measured ship plumes, see Figure 5.2. The EEPS underestimates the total number of particles by about 30 % as compared to the CPC results. Care has to be taken because the size limits of these two instruments are not identical. However, the measured number size distribution of particles emitted from ships as presented in Figure 8.2 indicates that the contribution of particles above 200 nm is negligible. The EEPS was cross-validated with the SMPS measuring ammonium sulfate particles at concentrations between $1.85 \cdot 10^5$ particles/cm³ and $8.36 \cdot 10^5$ particles/cm³. For ammonium sulfate particles with diameters around 30 nm it was found that the EEPS underestimates the particle size by approximately 14 % with respect to the evaluated geometric mean diameters (GMD). On the other hand, the found mode diameters indicate an overestimation of particle diameters by the EEPS between 9 % and 22 %, with an increasing deviation

for higher total concentrations. The difference in findings between the GMD and the mode diameters is due to the discontinuous behavior which can occur in the size distributions measured with the EEPS for particle diameters below 25 nm. In contrast to the distributions measured with the SMPS there appears to be a small peak around 10 nm and a dip around around 22 nm. Similar observations were reported by Jeong and Evans [2009] and Asbach et al. [2009]. Altogether, the uncertainties in the found size distributions compare well with the reported discrepancies by Kaminski et al. [2013]. The correction scheme suggested by Zimmerman et al. [2015] was not applied in these studies, yet. There is a need for further more rigorous validation of the EEPS. So we plan own comparison studies with SMPS for particles emitted from ship engines in the near future.

5.4 Analysis of particle composition

In this study, the sampled aerosol was stored in the liquid phase and analyzed for sulfates using ion chromatography which was conducted in the laboratory at a later stage.

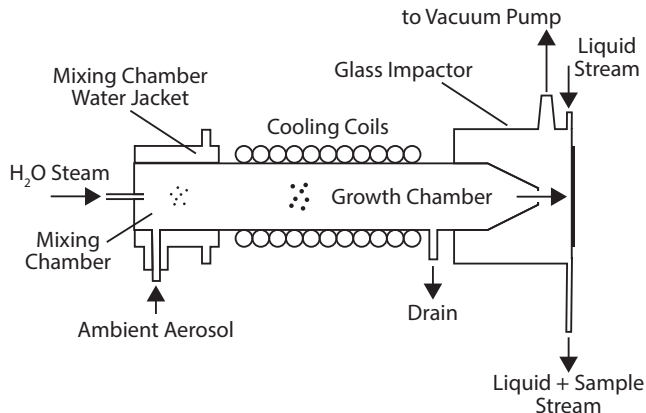


Figure 5.3: Principle of PILS (adapted from Weber et al. [2001]).

Particles are collected for later analysis of their composition using a **particle into liquid sampler (PILS)** [Weber et al., 2001, Orsini et al., 2003, Sorooshian et al., 2006]. Similar to a water-based CPC, particles pass through a supersaturated environment and function as vapor seeds. At first, large particles as well as organic, acidic and alkaline gases that can dissolve into water and create sampling artifacts are removed. Then the remaining particles are grown to droplets which impact on a collector which is continuously rinsed by a stream of distilled water taking up sampled particles. The ions in the sampled liquid can be analyzed directly if the PILS is run in

series with an ion chromatograph but the liquid can also be stored in small vials for later analysis. The PILS acts as a concentrator because the flow of the sampled air is in the order of 10 LPM while the flow of the up-taking liquid is only a few mLPM. Thus concentration ratios in the order of 10,000:1 are reached. The slow flow of the liquid also requires the sample to be taken for a certain period to gain enough liquid for the analysis. It should be noted that only water soluble particles, i.e. ions such as sulfate, can be collected.

A Brechtel PILS 4000 was used. From the results of Orsini et al. [2003] on this sampler, it can be seen that the collection efficiency is close to 100% for particles down to at least 30 nm. An aerosol mass spectrometer (AMS) was considered as an alternative method for the composition analysis, but its collection efficiency drops below 50% for particles below 50 nm [Jayne et al., 2000]. Unfortunately, this is exactly the size region that is of particular interest for sulfate measurements. Murphy et al. [2009] operated the PILS and the AMS in parallel during their measurements. The comparison of sulfate measurements indicated a collection efficiency of the AMS of 0.5 based on the PILS results, yielding a correction factor of 2 which they applied to achieve an agreement in their sulfate measurements.

An ion chromatograph was used to analyze the sulfate and other ions collected by the PILS. In **ion chromatography (IC)**, the sample liquid is introduced into an eluent which is moved through a chromatographic column. The sample ions interact differently with ions in the column wall, due to their specific affinities, which in turn makes them pass with different speed through the column hence making it possible to separate, identify and quantify them. In this project, two ICs were used, one for either, anion and cation measurements. The IC instrumentation is handled best under laboratory conditions with moderate temperature stability. Furthermore, the analysis time for each sample is several minutes. Calibration runs with multi-standards for both anions and cations, composed of several species at known concentrations, are needed. The manufacturer specified concentrations were diluted and measured in several steps.

In this study the PILS was operated together with an auto-collector that fills and stores the sample liquid into individual vials for each plume and back- ground measurement. The sampled liquids were analyzed with the ICs at a later stage in the laboratory. The PILS was tested for measurements of individual ships both from two helicopters (Neva Bay and North Sea), a harbor vessel in Neva bay and a fixed site at the harbor inlet to Göteborg. However, the sensitivity of the analysis was not good enough for measurements of individual ships, due to the short duration of the ship plumes. Instead a capturing volume, the multiple exhaust gas analyzer (MEGA)-chamber presented in **Paper E**, was employed with good results.

Chapter 6

Optical measurements

In Chapter 3, the overall measurement approach was described, including sniffer and optical measurements based on optical absorption measurements in the UV-visible range. The overall advantage with the latter method is that it possible to measure gas emissions from ships from higher altitudes between 200 and 300 m, than for the sniffer method which requires flying at altitudes between 50 and 100 m. This makes the compliance monitoring more efficient, but also less accurate compared to the sniffer technique. The optical method can also be employed from the ground for the estimation of the absolute ship emissions in grams per second in contrast to the sniffer method which yields emission factors in grams of pollutant per grams of fuel. The background, realization, and results of the optical measurements are discussed in the following sections of this chapter.

6.1 Theory

The basics of differential analysis in the UV/visible region of the optical spectrum reach back as to the 1920's, when Dobson used the idea of differential retrieval to determine the amount of ozone in the atmosphere [Dobson and Harrison, 1926]. Later this method, named Differential Optical Absorption Spectroscopy (DOAS), was improved and modified to the current state of the art technology [Platt and Perner, 1983, Platt and Stutz, 2008].

The Beer-Lambert law describes the absorption of light when it traverses through a homogeneous medium. The intensity of the light I falls exponentially with respect to an initial intensity I_0 depending on the length L of the path through a medium with the absorption cross section σ and assuming uniform concentration c :

$$I(\lambda) = I_0(\lambda) \cdot \exp(-\sigma(\lambda) \cdot c \cdot L) \quad (6.1)$$

The absorbing media is usually composed of several absorbing species at different concentrations c_i and with molecule-specific cross sections σ_i . Further, Rayleigh and Mie scattering by particles contribute to the extinction of light in the optical path

and can be described by the wavelength dependent extinction coefficients $\varepsilon_{Ray}(\lambda)$ and $\varepsilon_{Mie}(\lambda)$, respectively. Contributions to the extinction by the instrument can be described as an additional wavelength dependent factor $A(\lambda)$. Thus, Eq. (6.1) can be reformulated as

$$I_\lambda = I_{0,\lambda} \cdot \exp\left(-L \cdot \sum_i (\sigma_i(\lambda) \cdot c_i) + \varepsilon_{Ray}(\lambda) + \varepsilon_{Mie}(\lambda)\right) \cdot A(\lambda). \quad (6.2)$$

The intensity I_0 , which includes for instance the emitted spectrum of the radiation source, is not known. Further, the typical atmosphere consists of many species that might be absorbing in a certain spectral region, or Mie and Rayleigh scattering which contribute to the extinction of light. There are different ways to tackle the problems mentioned here, but one way is to assume that the slowly varying atmospheric scattering and background spectrum I_0 as well as instrument function A can be described by a polynomial of a few orders and then solve the corresponding inverse equation to Eq. (6.2) for the concentration of the key pollutants c_i by multivariate fitting using this assumption.

Another more common way is to explicitly use differential spectroscopy in which a discrimination between slow and fast variations with the wavelength is done in both, the measured spectra as well as for the calibration cross section spectra as shown in Eq. (6.3). The rationale behind this is that scattering effects due to Mie, $\lambda^{-(1...3)}$, and Rayleigh, λ^{-4} , scattering and the variation in the background intensity show a smooth variation while most of the absorption features of the species of interest show a faster variation versus wavelength [Platt and Stutz, 2008].

$$\tau' = \ln \frac{I_{0,S}(\lambda)}{I(\lambda)} = L \cdot \sum_i (\sigma'_i(\lambda) \cdot c_i). \quad (6.3)$$

Platt and Stutz [2008] show that the concentration of a specific gas c_i in the light path can be retrieved by solving Eq 6.3. Here the high pass filtered or differential optical depth, τ' , is obtained as the logarithm of the reciprocal ratio of the spectrum $I(\lambda)$ normalized with a low-order polynomial spectrum $I_{0,S}(\lambda)$. The differential optical depth in turn corresponds to a superposition of the differential absorption features of the absorbers obtained by high pass filtering, which is usually done by normalizing them with a low-order polynomial.

For a known path length L , the concentrations c_i of the contributing molecules can be calculated from the differential optical density by solving the corresponding inverse equation to Eq. (6.3) for the key pollutants by multivariate fitting. If L remains unknown, such as in passive measurements using natural light sources like the sun or the scattered sunlight of the sky, the product $c_i \cdot L$ is referred to as column density of the specific molecule and used as an equivalent quantity to the concentration.

6.2 Setup



Figure 6.1: Upward looking optical system. Here an upward looking telescope is connected an optical fiber which transmits light into a UV/visible spectrometer measuring wavelengths between 300 to 324 nm (courtesy of Jacob Balzani Lööv) .

The presented optical measurements in this work, **paper A**, were done in a static upward looking setup, see Figure 6.1, using DOAS methodology. To my knowledge, such measurements with focus to derive the emission rate in g/s from by passing emitters has not been carried out elsewhere. However, similar measurements have been carried out from moving platforms to measure industrial emissions [Johansson et al., 2008, Rivera et al., 2009, Johansson et al., 2014]. In this setup, used for ground-based measurements, a telescope is pointed upwards, collecting scattered skylight into a UV spectrometer via an optical fiber. The instrument is deployed downwind of passing ships, which ideally should move orthogonally to the wind direction, and the wind drives the plume across the telescope's field of view. In such way a profile of column densities along a cross section through the plume can be retrieved. The second setup is applied when measurements are taken from aircraft and the plumes are observed from above. The telescope is then pointed downwards with a certain angle to gather the skylight that is reflected and/or scattered at the sea-surface. At a flight track perpendicular to the plume, most of the light that reaches the telescope traversed through the plume twice; first when heading towards the sea-surface, second after reflection on the latter, heading upwards towards the telescope. Airborne measurements using DOAS techniques are thoroughly described by Berg [2011] and Berg et al. [2012].

As shown in Figure 6.2, the DOAS system consists of a telescope to collect the light

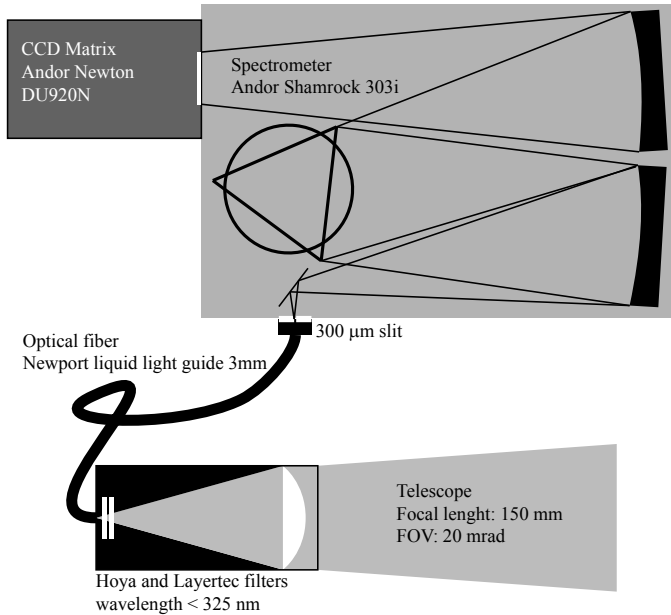


Figure 6.2: Basic setup of the DOAS system (courtesy of Niklas Berg).

with a certain field of view of, an optical fiber as a light guide into the spectrometer, a spectrometer to disperse the light and record its spectrum. The spectrograph (Andor Shamrock SR-303i) was used together with a UV enhanced CCD camera (Andor Newton 920BU) as detector. The focal length of the spectrograph is 303 mm. For the measurements of SO_2 , the selected grating had 2400 lines/mm and the slit was set to $300 \mu\text{m}$, to achieve a spectral resolution of 0.47 nm. The CCD detector has 1024 by 255 pixels, which were binned channel-wise. It is thermo-electrically cooled to -70°C to minimize noise. The $F/2$ telescope consists of a 75 mm quartz lens. Optical band pass filters in the telescope system were used to limit the spectral range and possible effects due to stray light in the spectrograph. The spectrograph and the telescope were connected by a liquid light guide with a core diameter of 3 mm. The field of view was hence 20 mrad.

6.3 Retrieval

The used spectral window for the DOAS retrieval of SO_2 was between 300 and 324 nm. The SO_2 molecules show strong absorption cross sections in this region but also over-

lap with the Hartley absorption bands of ozone. The recorded spectra were subtracted by the detector specific residual “dark” spectrum, that can be measured when no light hits the detector. The measured spectra were divided by a “sky” reference spectrum, which was recorded just before or after the emission plume was detected, in order to compensate for background concentrations and other spectral potential variations due to source or instrumentation.

The slant column density of SO₂ was determined according to Eq. (6.3) from multivariate fitting of low-pass filtered laboratory reference spectra that were adapted to the used instrument. However, there are other spectral structures in the selected spectral region that are not due to the absorption by SO₂ which have to be recognized. First, the absorption of ozone in this region was taken care of by including an ozone reference spectrum in the fit. Second, the Ring-effect due to inelastic rotational Raman scattering needs to be considered [Wagner et al., 2001]. A synthetic ring spectrum was calculated with the software DOASIS [Kraus, 2006]. The reference spectra, which are obtained from published data, have to be adapted to the spectrometer in use before the multivariate fitting. The spectral resolution of this instrument is limited by the finite width of the entrance slit of the spectrograph and as a consequence monochromatic light is dispersed over the detector area with a certain distribution which is referred to as slit function. The reference spectra, which are provided in high resolution, are convolved with the slit function in order to obtain reference spectra that can be fitted with the recorded spectra. The column densities of SO₂ were retrieved from the fitting with the WinDOAS software [Fayt and Van Roozendael, 2001].

By using the retrieved slant column densities and the knowledge about the wind speed, the actual emission flux f in kg/s can be calculated by

$$f = v_{aw} \cdot k_{\perp} \cdot k_{AMF} \cdot M(\text{SO}_2)/N_A \cdot \int c_i \cdot L \, ds, \quad (6.4)$$

where v_{aw} is the apparent wind speed, k_{\perp} corrects for the deviation between the direction of the actual traverse through the plume to the normal of the plume direction, and k_{AMF} is the air mass factor which corrects for the deviations in air mass if the telescope is not looking towards zenith. As such k_{AMF} is 1 for the case of the conducted ground-based, upward looking measurements. The factor $M(\text{SO}_2)/N_A$, with N_A as the Avogadro constant, converts number of SO₂ molecules to the corresponding mass. The column density is integrated over ds , which corresponds to the time between two scans times the speed at which the plume crosses the line of sight of the telescope [Berg, 2011, Johansson et al., 2014].

The relative uncertainties found for the upward looking measurements described in **Paper A** were about 10 % to 30 %. This matches well with the uncertainties found by Johansson et al. [2014] between 16 % and 34 % who presented an extensive uncertainty analysis for the measurement of SO₂ and other species for a similar instrumentation and setup as used for our measurements. Major sources of the overall uncertainty in the flux measurements are uncertainties in the retrieved wind speed and direction.

In downward looking, airborne DOAS measurements, the radiative transfer is slightly more complex as the influence of the sea surface, e.g. waves and sun glint does need to be accounted for. A thorough discussion about the uncertainties in the flux measurements of ship emissions for airborne measurements using back-scattered skylight from the sea-surface is presented in Berg et al. [2012]. They found an uncertainty for airborne DOAS measurements of SO_2 to be in the order of 30 % to 45 %.

Chapter 7

Aircraft installation

As mentioned in Chapter 2, this thesis work is an integrated part of the Swedish project IGPS-plus Mellqvist et al. [2014]. Within this larger project, a modular mobile measurement system, adapted for airborne use, has been developed and tested to measure ship emissions. The focus was on building a flexible system, capable of measuring multiple pollutants and which could easily be mounted/unmounted onto the aircraft. One of the modules should also be a self sustained basic system for compliance control of FSC, optimized for form factor, weight and power consumption, to facilitate installation in small aircrafts.



Figure 7.1: The Navajo Piper airplane with certified, permanent installation of the airborne IGPS system (courtesy of Tue Friis-Hansen).

The IGPS measurement equipment was permanently installed in a Piper Navajo Aircraft, Figure 7.1, operated by the Danish Aircraft ApS. This also required modification of the aircraft. For this installation, an approval for the modification of the aircraft had to be requested from the European Air Safety Agency (EASA) and this was obtained in December 2014 (Supplemental Type Certificate 10051623). The preparatory

work for the approval required extensive activities by a certified design and production organization and the design of dedicated IGPS instruments.

The modified Piper Navajo airplane has previously been commissioned for oil spill reconnaissance to the Swedish Coast Guard. It is a low-winged, twin-engined aircraft, and the latter is beneficial for the sake of safety when measuring in open sea. In its standard configuration it is equipped with seats for four passengers, but to make space for the instrument racks three of the passenger seats had to be removed. Here a brief description of the airplane installation is given and more information is given in Mellqvist et al. [2014].

7.1 Instrument racks and probe plate

Three instrument racks and a window probe plate has been installed in or the aircraft, respectively, in addition to some modifications on the airplane.

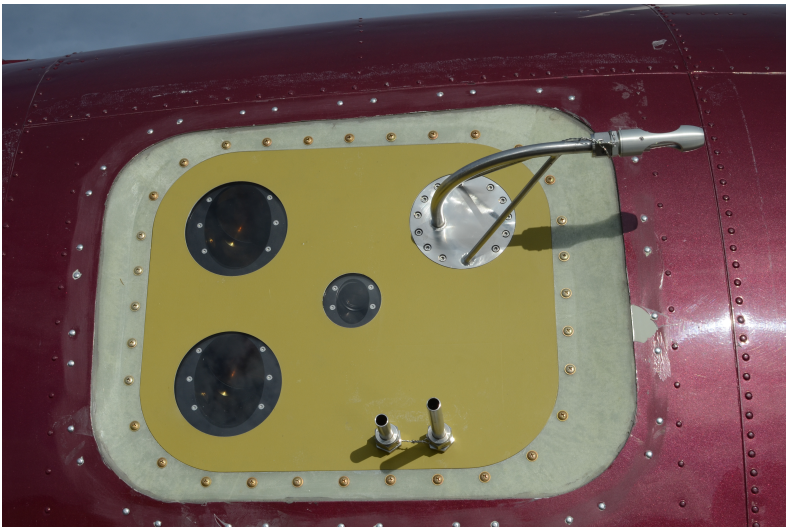


Figure 7.2: The window probe plate on which the gas and particle inlets for the sniffer measurements as well as common outlet are mounted. It also carries two telescopes and a video camera used for the optical measurements.

The window probe plate shown in Figure 7.2 replaces one of the airplane's windows and carries a gas inlet, a particle probe, a common gas outlet, two telescopes and a video camera. The probe plate is located behind the wing to provide an open field of view for the telescopes which are mounted looking downwards at a 30° angle with respect to the horizon in order to gain a sufficient amount of light for spectral analysis

[Berg et al., 2012]. The video camera will be used in future studies on the radiative transfer, which is affected by scattering in the plume and on the water surface, to derive the uncertainties in the effective light path through the plumes. It is mounted in the same orientation as the telescopes.

The racks carrying the ship emission equipment in the Piper Navajo aircraft, Figure 7.3, are designed in functional groups, i.e. one rack for sniffer measurement of gas species, one for particles and a third one for optical measurements of gases. The racks are interconnected to an in-system power bus at 115 V and an Ethernet interface for control and data communication.



Figure 7.3: The gas rack (right) contains instrumentation for measurements of CO_2 , SO_2 and NO_x as well as a buffer battery and the main computer. The particle rack (left) includes instrumentation to assess the exhaust aerosol's particle size distribution. SO_2 and NO_2 is also analyzed using the spectrometers in the optics rack (middle).

The gas rack is connected with the airplane's avionic data bus (ARINC 429) and also includes the main computing unit which is also used for logging all data. It is also connected to an AIS and a GPS antenna. The main computing unit also processes the wind data, delivered from the airplane's own instrumentation, to control the airflow for the flow through the aerosol inlet. Some of the instruments need a warm-up time of about 30 to 60 min, during which they can be supplied from ground power. However, a buffer is needed for the transition time between the shut-off ground and availability of aircraft power. Hence, the gas rack also includes a buffer battery to overcome the power gap. It's capacity is sufficient to run the critical set of instruments regarding warm-up time, for about 20 minutes to keep them ready and stabilized for the mea-

surements.

The gas rack contains a compact basic module for measurements of CO_2 and SO_2 , including the main computing unit, which together with the buffer battery is sufficient for the FSC monitoring task. The gas rack in addition contains a chemiluminescence instrument (Thermo 42i-TL) for NO_x and a CRDS (Piccaro G2301-m) for CO_2 analysis, to improve accuracy and the need for frequent calibrations in the air.

The particle rack is placed next to the probe plate to keep the inlet tubing as short and straight as possible to minimize losses. It contains the EEPS and OPS particle sizers which together covers particle size measurement in the range from a few nm to $10\ \mu\text{m}$. Particle measurements, are sensitive to differences between the airspeed at the particle inlet outside the airplane and the flow at the inlet, with effects to the sampled particle size distributions and the functionality of certain instruments. Especially the OPS showed to be sensitive to the sample flow which was noticed on the measurements conducted from Kiel (**Paper B**). To obtain an undisturbed isokinetic flow at the tip of the inlet, the inlet is adapted to the airspeed [Hinds, 1999].

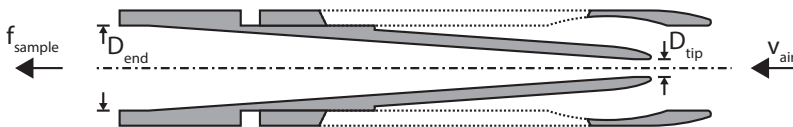


Figure 7.4: Solid Diffuser Aerosol Inlet developed by A. D. Clarke, University of Hawaii.

The aerosol probe outside the aircraft, Figure 7.4, is based on a solid diffuser design developed by A. D. Clarke, University of Hawaii [Huebert et al., 2004, McNaughton et al., 2007]. In the probe, the air flow is slowed down by a gradual widening of the inner diameter of the probe tube to match the sample flow of the pump. The inlet is connected to a splitter which divides the flow for the particle sizers and the pump. The particle tubes to the instruments are kept as straight and vertical as possible to minimize diffusion and settling losses.

There are two spectrometers enclosed into the optics rack (Andor SR-163 and SR-303) equipped with thermo-electrically cooled CCD cameras (Andor Newton 920DU). This allows for simultaneous measurements of SO_2 and NO_2 at two different wavelength regions, i.e. around 311 nm and 450 nm, respectively. The spectrometers are connected to two separate telescopes, both with a focal length of 150 mm. The comparatively long focal lengths of the spectrometers (163 and 303 mm) allow to use large slit widths to gain more light and still achieving a good spectral resolution. This is important for the downward looking measurements as the intensity of the reflected sky light from

the sea surface is rather weak. The optics rack also includes a computer for controlling the spectrometers and logging the spectra.

As part of the approval process for the flight certification, all racks were tested regarding electromagnetic interference and magnetic properties (RTC DO 160/issue M/cat M/section 21 and section 15). Further, components made of PVC were removed as much as possible to reduce the risk of toxic hydrogen chlorine production in the case of fire. Additionally, halon-based fire extinguisher cartridges were installed in some of the instrument boxes.

7.2 Operation



Figure 7.5: One window probe plate and three instrument racks for ship emission measurements in a Navajo Piper airplane.

The installation of the instrument racks and window probe plate in the Navajo Piper aircraft are shown in Figure 7.5. The system can be operated by a single person. The measured concentrations of the pollutants by the sniffer instruments are presented in real-time to the operator. In addition, the encountered ship plumes are detected automatically and the FSC and specific NO_x emission factors are evaluated in semi-real-time by the in-house developed software “IGPS Real”. The user interface shown in Figure 7.6, supports the operator in choosing vessels of potential interest and also calculates the location of the emission plume to assist the navigation. The column density data from the optical measurements is also given in real-time but for each plume transect, the measurements are restarted to obtain a reference spectrum which is taken at similar light conditions as in the ship plume. In the future it is foreseen that the optical software will be more automatic, not requiring manual starting and stopping as it currently does. The results of the optical measurement can be used as an indicator whether the ships are running on high or low FSC and whether further

analysis with sniffer measurements should be carried out.

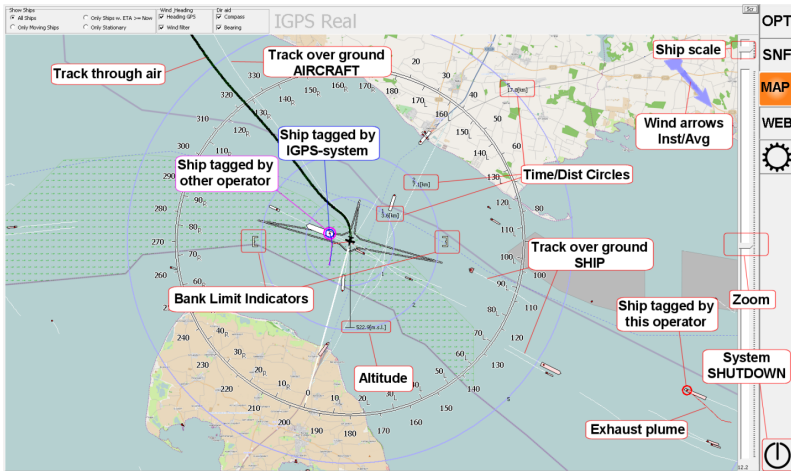


Figure 7.6: User interface of the control and logging software “IGPS-real”, which was developed within the IGPS project. The software uses information from the AIS and GPS receivers as well as information from the air data computer about wind speed and direction to plot the locations of the aircraft, ships and their exhaust plumes (map data: OpenStreetMap, 2014).

Chapter 8

Results

The results presented in this chapter are a brief compilation of the findings presented in the appended papers. In addition new results are presented regarding the correlation between emitted particles and SO₂.

8.1 Effect of IMO regulation on SO₂ emissions from ships

The measurements in this study were conducted in the European SECA regions with the FSC limits as given in Figure 2.1, i.e. 1.5 % FSC until mid 2010 and subsequently 1 % until the 0.1 % limit came into effect since the beginning of 2015. In Figure 8.1, results from **Paper B** and **Paper D** are shown as histograms of the retrieved FSCs for ships at open-sea measured from aircraft and ships passing the fixed station at the harbor entrance of Gothenburg for periods before and after the change in FSC in 2010. The measurements in 2007 were conducted during 14 days and 74 ships were measured about 3 times on average, while for the period between 2012 and 2014 the presented measurements were carried out on 304 days between September 2012 until December 2014, when 408 ships measured 7 times on average. It is clear that there was a large shift towards lower FSCs between 2007 and 2012. In addition, more than 95 % of the ships measured in Gothenburg appear to be compliant with the IMO sulfur limits, taking into account the measurement uncertainties of around 20 %. A bi-modal distribution can be seen for the years 2012 to 2014, with one peak around 0.7 % and a second one around 0.1 %. The ships that are contributing to the latter peak are tug boats and smaller tankers, up to 2,000 gross tons. The port of Gothenburg encouraged ship owners to use fuel with sulfur contents of 0.1 % even before the official fuel switch to this level in January 2015. The effect can be seen in this distribution. Further results of the measurements conducted in Gothenburg harbor and the according discussion can be found in **Paper D**. Here the significant reduction of the FSC in the used bunker fuels can be seen from measurements conducted during the first 18 days of January 2015 which is in accordance with the recent introduction of the new lower sulfur limit. From the presented results, it can be seen that the monitored ships use

low sulfur fuel of some kind but that several are not yet compliant with new regulation.

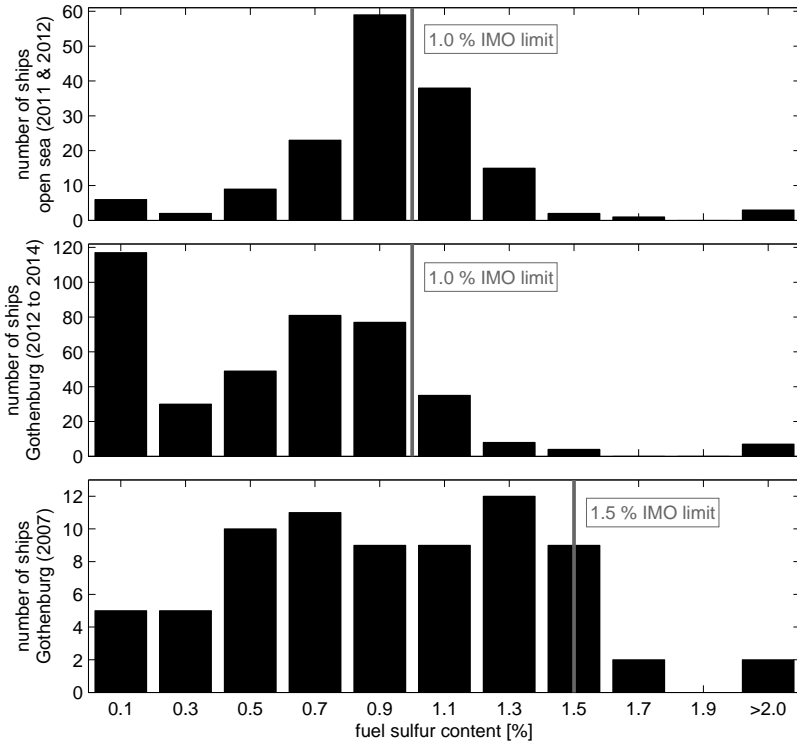


Figure 8.1: Measured FSCs of ships passing the harbor entrance of Gothenburg and at open-sea. The harbor measurements are based on measurements in 2007 (14 days) and during the measurement period between 2012 and 2014 (304 days). The airborne measurements at open sea were conducted during field campaigns in 2011 and 2012 (25 days).

Airborne measurements are mainly intended for compliance control and mostly international going ships are monitored. The measurements presented in Figure 8.1 took place in the Baltic and North Sea in 2010 and 2012, and they are described in detail in **Paper B**. A clear distinct peak in the distribution can be observed around the IMO limit of 1 %. This is slightly higher than the peak found from the passive measurements at the fixed monitoring site in Gothenburg. The difference is probably due to the arbitrary selection ships to be monitored during the flights, i.e. mostly bigger cargo ships and tankers, whereas for the measurements in the harbor a comparatively higher fraction of smaller and more regional vessels was seen monitored from the fixed site. The comparison with to earlier conducted airborne measurements

shows a general reduction in the used FSC after the fuel switch to 1 % as was also seen in the fixed-site harbor measurements in **Paper D**. The compliance level at the open sea in 2011/2012 is about 85 %, hence lower than the compliance found for the measurements at the harbor entrance of Gothenburg.

8.2 Particle emissions and their relation to the sulfur content

A fraction of the sulfur in the ship exhaust plumes is present as sulfate particles as briefly discussed in Chapter 5. This leads to an underestimation of the measured FSC by using Eq. (4.2), since it is based on the assumption that all sulfur is emitted as SO_2 . To investigate this, the gas phase measurements were complemented by aerosol measurements.

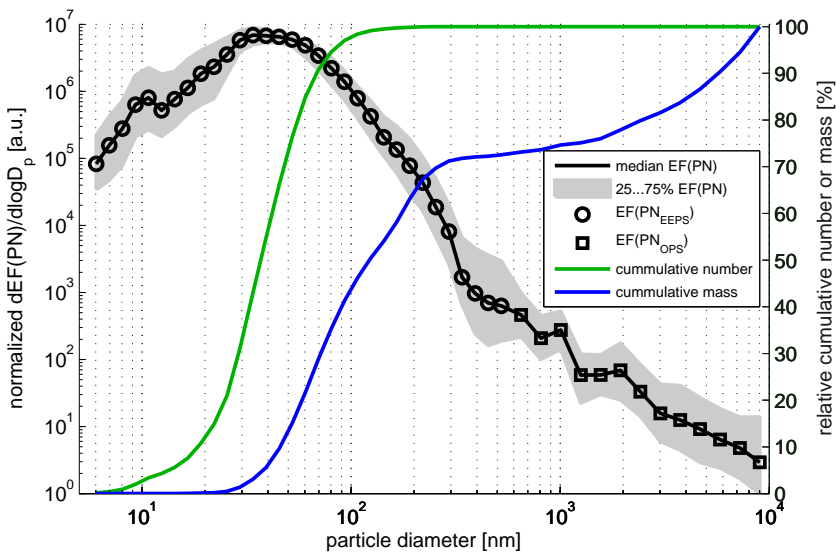


Figure 8.2: Averaged and normalized size and mass distributions of the measured emission factors of the particle number.

Measurements of the total number of particles as well as number and mass size distributions were conducted in the Neva Bay region covering a broad range of ship types and dimensions, going on international and inland waters. Most of the ships that were monitored were running at reduced speed, but under stable load conditions. These results are presented in detail in **Paper C**. The averaged and normalized number size distribution of particles is shown in Figure 8.2. Concerning particle number, it can be seen that nearly all emitted particles are smaller than 100 nm. Two modes can be seen

in this size region, one around 10 nm and another which peaks between 20 and 70 nm, whereof the mode at 10 nm should be regarded with according to the discussion in Section 5.3. The density of the particles is not known, hence a unit density ($1\text{g}/\text{cm}^3$) is assumed over the entire size range. It was found that about 70 % of the total mass is due to particles below 300 nm. Concerning the presented particle sizes, it should be considered that they are measured by two different methods. Particles with sizes up to 560 nm were measured with the EEPS and thus characterized by their electro-mobility while the bigger particles up to $10\ \mu\text{m}$ are characterized using their optical properties.

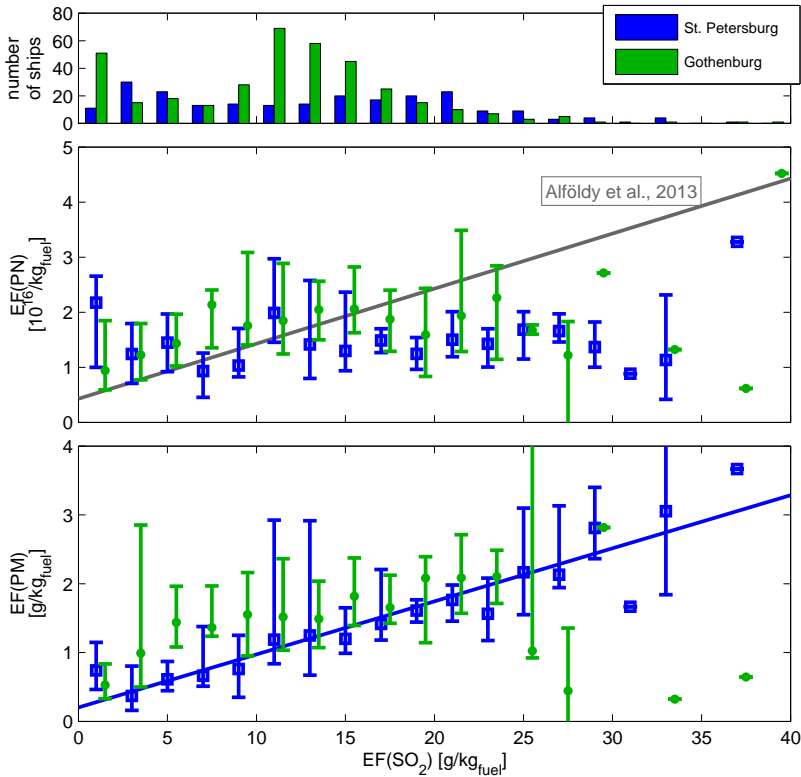


Figure 8.3: SO_2 dependence of emission factors of particle number, $\text{EF}(\text{PN})$, and particle mass, $\text{EF}(\text{PM})$. The results are binned over $\text{EF}(\text{SO}_2)$ with a bin width of $2\ \text{g}_{\text{SO}_2}/\text{kg}_{\text{fuel}}$. The results for Gothenburg are plotted with an $\text{EF}(\text{SO}_2)$ offset of $0.5\ \text{g}_{\text{SO}_2}/\text{kg}_{\text{fuel}}$ for clarification. The error bars show the binned median values with the 1st and 3rd quartiles. The particle number is compared to the regression found by Alföldy et al. [2013] (grey line). The blue line is the regression ($R^2 = 0.85$) for the St. Petersburg with $\text{EF}(\text{PM}) = 77.1\ \text{mg}/\text{g}_{\text{SO}_2} \cdot \text{EF}(\text{SO}_2)\ \text{g}_{\text{SO}_2}/\text{kg}_{\text{fuel}} + 201.6\ \text{mg}/\text{kg}_{\text{fuel}}$.

In Figure 8.3, unique results for Neva Bay and Gothenburg harbor are shown for

averaged emission factors of particle number and mass versus the emission factors of SO_2 . Note that the latter is proportional to the FSC. The measurements do not indicate a clear correlation between particulate number and FSC, as it was found by Alföldy et al. [2013], see their regression drawn in the figure, and as predicted by Buhaug et al. [2009], even though the ranges seem to match well. Instead there appears to be a correlation between the particle mass and the emitted SO_2 in the case for the measurements in Neva Bay although a similar correlation is not evident for measurements in Gothenburg harbor. This is currently not understood and a subject for further discussion. It could be argued that the data in Figure 8.3 has to be divided into similar type of ships to be able to see any correlations. This was however done but still with similar results as before. One reason for the poor correlation between particle number and FSC, for ships below FSC of 1 %, is that the sulfate particles only correspond to a limited fraction of the particles and that removing them therefore only has limited impact on the particle content. This is however not consistent with Alföldy et al. [2013] and Buhaug et al. [2009]. Diesch et al. [2013] recently showed a distinct correlation between organic particulates and the FSC for measurements of 139 ships plumes along the river Elbe and less correlation between sulfate and FSC. It was argued that the organic particles are formed from lubrication oil, and that the amount injected is proportional to the FSC. The results in **Paper E** show that the sulfate corresponded to 10 and 22 % of the total particle mass. Diesch et al. [2013] reported similar results from their measurements. One reason for the difference in correlation between PM and FSC in Neva Bay and Gothenburg could be the fact that the ships in the former location are running in steady state conditions, with low load, while in the latter one they are maneuvering, either accelerating or decelerating. The study of Winnes and Fridell [2010] supports the assumption that the particle emission of maneuvering ships cannot clearly be related to their FSC. Also other factors might contribute to a potential correlation, if there even is a first order relationship, which is a matter to be resolved in future.

Considering the missing sulfur for the FSC retrieval, sulfates are of particular interest. In the appended methodology **Paper E**, particle composition measurements of several individual ships in the harbor entrance of Gothenburg are described using a particle into liquid sampler (PILS) and subsequent ion chromatography analysis, combined with a fast large volume extraction chamber, denoted as multiple exhaust gas analyzer (MEGA)-chamber. Although the methodology has been demonstrated for only seven ships, the range of the results is consistent with the findings of Diesch et al. [2013] and show that only minor fraction of about 5 % of the total emitted sulfur in form of sulfate and SO_2 is emitted as sulfate. The data also indicate that a large fraction of the particles, above 50 %, is something else than sulfate and soot, presumably organic aerosols. Hence it appears that the influence of sulfates on the determination of FSC using Eq. (4.2) is limited. In **Paper A**, and **Paper D**, it is reported that there appears to be underestimation of about 10-20 % when determining the FSC using the SO_2 -to- CO_2 ratio. It appears that one third of this could be explained by the emission of sulfur in form of sulfate.

8.3 Optical analysis of SO₂ emissions

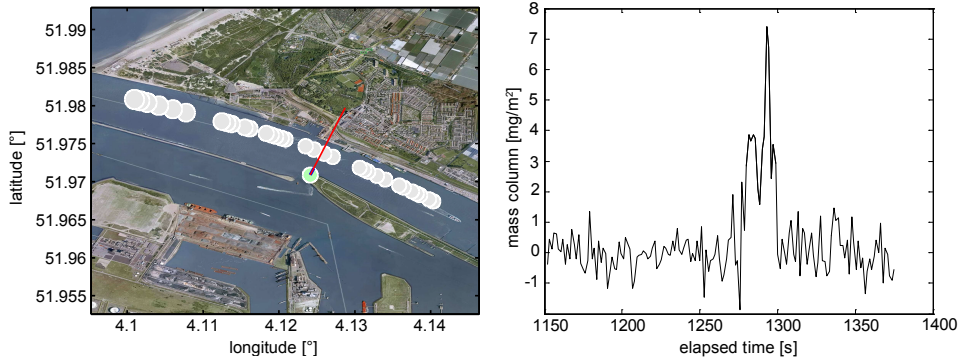


Figure 8.4: The left panel shows the location of the fixed measurement site (green circle), at the “Landtong” in the ship channel of Rotterdam, opposite to Hoek van Holland (map data: Google, 2010). The course of the passing ship “Autumn Wind” is shown (gray circles) and the wind direction is indicated by the red line. The corresponding retrieved mass columns of SO₂ are shown in the panel to the right.

Optical measurements using upward looking DOAS, as described in Chapter 6, were conducted in the ship channel of the port of Rotterdam on September 17 and 18, 2009. On the first day a fixed measurement site was used, at the Landtong across from Hoek van Holland, and the exhaust plumes of the passing ships which drifted across the field of view of the instrument were measured. On the second day the system was placed on-board a pilot vessel “RPA 16” which was operated downwind of the ship channel outside Rotterdam, to capture the plumes in the same manner as at the fixed site. This method works best when the wind direction is perpendicular to the direction of the ship movement. Information about the ships’ current positions and speeds was retrieved from the received AIS signal. An example of such measurement is shown in Figure 8.4. The wind was measured locally simultaneously with the measurements. The results of the measurements are presented in Table 8.1. The data here correspond to the estimated emission from several ships. The overall range of the obtained results was compared to other optical remote sensing methods such as differential absorption LIDAR (DIAL) and the UVGasCam [Prata, 2014]. The emission rates of SO₂ from ships were retrieved with DOAS and DIAL agreed relatively well while the UVGasCam significantly higher emission rates. These results contributed to **Paper A**.

Table 8.1: Measured SO₂ fluxes from the upward looking DOAS measurements.

Ship name	IMO	Type	DWT	DOB	SOG [kn]	mean flux [kg/h]	Rel. σ [%]
Stena Hollandica	9145176	ROPAX	10670	2001	9.9	91.1	11
Stolt Cormorant	9148960	Tanker	5498	1999	11.2	8.7	13
Autumn Wind	9038323	Reefer	13981	1993	9.6	11.3	13
Stena Britannica	9235517	ROPAX	12200	2003	4.0	29.7	9
Maas Viking	9457165	Cargo	11636	2009	17.1	36.7	30
Stena Hollandica	9145176	ROPAX	10670	2001	14.5	114.6	14
Hyundai Courage +2 Tugs	9347542	Container	99052	2008	7.9	17.2	19
Maersk Naantali	9312078	Tanker	16642	2005	11.1	9.7	25
CMA CGM Platon	9362437	Container	19430	2007	11.7	14.6	33
Stena Partner	7528635	ROPAX	6594	1978	15.7	26.5	32
Yu Lin Wan	9283277	Tanker	109181	2004	10.6	31.0	26

Chapter 9

Summary of appended papers

Appended to this thesis there are five papers, which are reflecting the scientific part of my PhD work. A brief summary is presented in the following.

A comparison study of different methods to determine the SO_2 and NO_x emissions from ships is presented in **Paper A**: *Field test of available methods to measure remotely SO_x and NO_x emissions from ships*. It took place in 2009 (sulfur limit was 1.5 % at that time) in Rotterdam under the lead of the European Commission's Joint Research Center (JRC) as part of their SIRENAS (Ship Investigation Remotely about NO_x and SO_2) field campaigns. Both, extractive and various optical methods were used to evaluate emission factors, FSC, and fluxes of the species of interest. Several European research groups were involved and measurements were simultaneously conducted for the inter-comparison of the different methods. Various stationary and mobile platforms, i.e. a boat and a helicopter were used during the course of the campaign. Further measurements were conducted on-board the RoPax vessel Stena Hollandica in conjunction with remote measurements of this ship. The differences and uncertainties of the applied methods are discussed in this paper. I contributed to this article by carrying out, analyzing and compiling the ground-based, upward-looking optical measurements.

The results of four airborne campaigns for emission measurements of ships at open sea are presented in **Paper B**: *Airborne emission measurements of SO_2 , NO_x and particles from individual ships using a sniffer technique*. The measurements covered the Western Baltic and the North Sea region in 2011 and 2012 (sulfur limit 1 %). The results here are representative for larger ships that were operated at steady speed, at optimal running conditions. The campaigns were conducted using different sniffer setups, sometimes measuring only emission factors of SO_2 . On three campaigns the SO_2 measurements were complemented by NO_x measurements, and on two campaigns additionally by particle size analyzers. More than 150 different ships were monitored during these campaigns. My part consisted of carrying out, analyzing and publishing the results from the measurements.

Two field campaigns were conducted in the Gulf of Finland close to St. Petersburg in 2011 and 2012. In these campaigns, emissions from both international and inland shipping were observed from fixed measurements on a port authority vessel that was anchored downwind the main shipping route in the Neva Bay and from different sites at shore. The results here are representative for large ferries and small to medium sized container and bulk ships, operating at steady speed, but low load running conditions. The ship fleet was a mixture of vessels operating in inland and international traffic, respectively. Both, gas and particulate matter emissions were measured simultaneously. Additionally, helicopter based measurements were conducted further out in the Gulf of Finland. The results from these campaigns are presented in **Paper C: *Emission factors of SO_2 , NO_x and particles from ships in Neva Bay from ground-based and helicopter-borne measurements and AIS-based modeling.*** I carried out, analyzed and disseminated the measurements

Paper D: *Remote Compliance Monitoring of Gas Emissions from Shipping to Enforce International Policies* is a summarizing methodological paper about the applied methods as tools for compliance control. Different strategies for remote compliance monitoring, from automated fixed site to mobile emission measurements, are discussed in this paper. The paper also presents new results from several years of monitoring at a fixed site in Gothenburg and the results nicely show the influence of the increasingly stricter sulfur regulations over the years. My part consisted of general instrument development, strategy planning, compilation and analysis of the results and their dissemination.

In **Paper E: *Characterisation of particle emissions from individual ships using plume catching by MEGA-chamber***, a method is presented to capture and analyze quickly passing plumes. This paper focuses on the analysis particle emissions from individual ships by combining a MEGA-chamber for the sampling of particulate matter and analyzing their composition using a PILS combined with ion chromatography. The methodology is illustrated by the measurement the exhaust of several ships at a fixed site in Gothenburg. In this paper, results about the particle composition, especially regarding sulfates are presented. I contributed to this work by acquiring and building up the equipment and assisting with the measurement, analysis and dissemination of the results.

Chapter 10

Conclusions

Emissions from shipping are currently a hot topic in the European SECA due to the new, stricter sulfur regulation which since the beginning of 2015 allows a maximum fuel sulfur content of only 0.1 %. Sniffer and optical systems have therefore been developed to be able to remotely monitor that the ships comply with international emission regulation. This includes an operative system for airborne emission monitoring of ships in a certified installation in a Navajo Piper and an automated system for fixed-site measurements.

In a joint comparison study comprising different methods for compliance monitoring, and by the experience gained from the field campaigns of this study, it has been shown that the sniffer technique is a suitable, and reliable tool to remotely monitor the FSC of individual ships and identify gross-polluters. In addition, optical measurements can complement the sniffer measurements to provide absolute emission rates and more efficient monitoring.

Sniffer instrumentation was developed for autonomous compliance monitoring from harbor vessels or fixed sites along ship passage ways. It was shown that the absolute uncertainty in the FSC measurement is 0.06 % for ships running 0.1 % FSC while somewhat larger, i.e. 0.2 % for ships running 1 % FSC. Part of the uncertainty is due to the fact that about 5 % of the sulfur is present in particulate form. This makes the technique reliable enough to discriminate between the use of high and low sulfur oil. The advantage with the fixed measurements is that they are fully automated and can provide data for the thousands of individual ships per year that enter harbors. The real-time data can be used to alert port state control authorities for further on board inspection and this is actually how the data is foreseen to be used in the near future. The worries about these measurements is that ship operators will learn about their position and adapt to these places. The airborne measurements, on the other hand, make it possible to measure ships in the open sea, where according to authorities the probability for running non-compliant fuel is largest. Since the aircraft measurements are conducted on short notice, ship crews will not have time to adapt by switching to

compliant fuel. On the other hand, the operation of an aircraft is expensive as about up to 10 ships per hour can be monitored but at a cost of several thousand Euros.

Optical measurements using DOAS are applicable in different ways. First, optical methods can be used at fixed sites to estimate the absolute ship emission, given that the wind transports the ship plume across the fixed site. Secondly, optical methods for the analysis of SO₂ and NO₂ can be used in airborne measurements to locate ship plumes from altitudes between 200 and 300 m and can, in conjunction with modeled CO₂ emissions, provide a first estimate of the FSC in the bunker fuel of studied ship. If a first indication of too high FSC is given for a ship, it can further be controlled by the more accurate sniffer measurements conducted at lower altitudes, between 50 to 100 m.

The evaluation of the ships' compliance to the IMO's regulation on NO_x emissions is harder to evaluate by remote measurements of the exhaust. It is engine specific and on bigger ships there are several main and auxiliary engines contributing to the total emission of NO_x. For airborne measurements, the uncertainty of the emission factor of NO_x related to the consumed fuel oil is about 25 % and the uncertainty for the brake specific emission factor of NO_x is about 30 %. However, remote measurements are certainly a suitable tool to monitor the compliance for the coming generation of vessels going under the MARPOL tier 3 limits. These vessels have to use highly-effective reduction techniques and the emission factor of NO_x in the cleaned exhaust will be significantly below those with no active reduction.

In this study, ships going in international traffic and inland traffic were observed in different environments and as such in different operation states; at open-sea (steady-state, optimum), harbor areas (maneuvering) and speed-reduced passage ways (steady-state, non-optimum). For instance, for ships in international traffic on open sea average emissions of about 18.8 ± 6.5 gSO₂/kg_{fuel}, 66.6 ± 23.4 gNO_x/kg_{fuel} and 2.8 ± 1.6 mg_{PM}/kg_{fuel} were measured in the years 2011 and 2012. The compliance with respect to the IMO limits by these ships was about 85 %. This can be compared to the compliance by ships which were maneuvering in low load condition in the Neva Bay which was found to be 90 % and 97 % for measurements in summer 2011 and summer 2012, respectively.

When comparing modeled ship emission with the measurements, it was found that inland vessels used fuel with considerable lower FSC than assumed in the model. The measured NO_x emissions seem to agree well with the model results, while modeled particle emissions deviated significantly from the measured results, potentially due to the differences of assumed for the FSC in the model to the real values.

Chapter 11

Outlook

Compliance monitoring is currently of major interest in SECAs, but from 2020 on there will be a worldwide 0.5 % limit for the FSC. NO_x ECAs (NECA) will be adapted around the US from 2016 and some years later also in northern Europe. This implicates that there will be an increasing need for (airborne) compliance monitoring of FSCs and soon also emission of NO_x to assure a level playing field.

It will be interesting to follow the development of particle emissions. The results of our measurements indicate that the reduction of the FSC will result in only little improvement in the overall particle loading. This remains to be examined during this year since the FSC limit now has been significantly decreased. Black carbon from shipping will become a matter of increasing interest, as arctic shipping is becoming an economically tempting alternative as ship routes. We plan to carry out measurements of black carbon by our own instrumentation.

There is a need to further investigate the gas and particle emissions from ships using abatement techniques, such as selective catalytic reduction (SCR) techniques or scrubbers, or run on alternative fuel like LNG or methanol.

Concerning the instrumentation used in this project, the following technical improvements should be carried out in the near future.

The analysis of particulate matter needs further attention. The reliability of the EEPS is currently in question and needs to be validated more extensively. Parallel measurements of exhausts from ship engines using the EEPS together with a SMPS and a CPC are needed and will be conducted in the near future.

Further, additional work and studies are also needed connected to plume capturing using the presented MEGA chamber. Right now this chamber is operated fully manually, but the plan is to automate the shutters and use the gas signal as a tracer for plumes, such that the capturing can be triggered automatically or at least remotely as

the current measurement site is located on an island and not easy to reach. Further investigations are needed concerning dilution and effects due to plume aging.

The airborne measurement setup comprising a complete set of instrumentation for gas phase, sniffer and optical, and particle sizers was recently certified and it is now ready for compliance monitoring tasks. Additional data will be collected in future flight campaigns to improve the understanding of the radiative transfer and to provide a better understanding of the uncertainties using airborne optical measurements to analyze plumes using the reflected light from the sea-surface.

Chapter 12

Acknowledgments

I would like to express how much I have appreciated the last five years with all its big and small adventures, ups and downs; as many as you can have, when conducting airborne measurements with repeated altitude changes. First, I would like to acknowledge my supervisor Johan Mellqvist and co-supervisor Bo Galle. Johan, I want to give you my sincere gratitude for making this very applied and exciting project possible. I'm really looking forward to the field campaigns that are about to come.

This project was teamwork at its best and it would not have been possible to conduct it like this without the programming and engineering skills of Johan Ekholm, nor without Kent Salo's expertise on particulate matter. I would like to thank Tue Friis Hansen for providing us with his airplane as a measurement platform and for his piloting during countless flight hours. Thanks are also directed to all the other people and groups throughout Europe, who were involved in the preparation and conduction of the measurements.

Special thanks are also directed to all current and former members of the Optical Remote Sensing Group for fruitful discussions and assistance whenever needed. I also would like to thank my friends as well as my colleagues in the Department of Earth and Space Sciences for creating a highly enjoyable atmosphere at work and beyond.

At last, I would like to deeply thank my family; I know, I can always rely on you!

Jörg Beecken
Gothenburg, January 2015

REFERENCES

- B. Alföldy, J. B. Lööv, F. Lagler, J. Mellqvist, N. Berg, J. Beecken, H. Weststrate, J. Duyzer, L. Bencs, B. Horemans, F. Cavalli, J. P. Putaud, G. Janssens-Maenhout, A. P. Csordás, R. Van Grieken, A. Borowiak, and J. Hjorth. Measurements of air pollution emission factors for marine transportation in seca. *Atmospheric Measurement Techniques*, 6(7):1777–1791, 2013.
- M. Anderson, K. Salo, T. M. Hallquist, and E. Fridell. Characterization of particles from a marine engine operating at low loads. *Atmospheric Environment*, 101:65–71, 2015.
- C. Asbach, H. Kaminski, H. Fissan, C. Monz, D. Dahmann, S. Müllhopt, H. R. Paur, H. J. Kiesling, F. Herrmann, M. Voetz, and T. A. J. Kuhlbusch. Comparison of four mobility particle sizers with different time resolution for stationary exposure measurements. *Journal of Nanoparticle Research*, 11(7):1593–1609, 2009.
- N. Berg. *Remote measurements of ship emissions*. Technical report. 1, 43, 2011. Licentiatavhandling, Göteborg: Chalmers tekniska högskola, 2011.
- N. Berg, J. Mellqvist, J.-P. Jalkanen, and J. Balzani. Ship emissions of SO₂ and NO₂: DOAS measurements from airborne platforms. *Atmos. Meas. Tech.*, 5(5):1085–1098, 2012. ISSN 1867-8548. doi: 10.5194/amt-5-1085-2012. URL <http://www.atmos-meas-tech.net/5/1085/2012/http://www.atmos-meas-tech.net/5/1085/2012/amt-5-1085-2012.pdf>. AMT.
- Ø. Buhaug, J.J. Corbett, Ø. Endresen, V. Eyring, J. Faber, S. Hanayama, D.S. Lee, D. Lee, H. Lindstad, A.Z. Markowska, A. Mjelde, D. Nelissen, J. Nilsen, C. Pålsson, J.J. Winebrake, W.-Q. Wu, and K. Yoshida. Second IMO GHG study, 2009. Report, International Maritime Organization (IMO) London, UK, April 2009.
- G. Burba, D. McDermitt, D. Anderson, M. Furtaw, and R. D. Eckles. Novel design of an enclosed CO₂/H₂O gas analyser for eddy covariance flux measurements. *Tellus B*, 62(5), 2011. ISSN 1600-0889. URL <http://www.tellusb.net/index.php/tellusb/article/view/16629>.
- G. Chen, L.G. Huey, M. Trainer, D. Nicks, J. Corbett, T. Ryerson, D. Parrish, J.A. Neuman, J. Nowak, D. Tanner, J. Holloway, C. Brock, J. Crawford, J.R. Olson, A. Sullivan, R. Weber, S. Schauffler, S. Donnelly, E. Atlas, J. Roberts, F. Flocke, G. Hübler, and F. Fehsenfeld. An investigation of the chemistry of ship emission plumes during itct 2002. *Journal of Geophysical Research D: Atmospheres*, 110(10): 1–15, 2005.
- H. Chen, J. Winderlich, C. Gerbig, A. Hofer, C. W. Rella, E. R. Crosson, A. D. Van Pelt, J. Steinbach, O. Kolle, V. Beck, B. C. Daube, E. W. Gottlieb, V. Y. Chow, G. W. Santoni, and S. C. Wofsy. High-accuracy continuous airborne measurements of greenhouse gases (CO₂ and CH₄) using the cavity ring-down spectroscopy (CRDS) technique. *Atmospheric Measurement Techniques*, 3(2):375–386, 2010.

- J. J. Corbett and P. Fischbeck. Emissions from ships. *Science*, 278(5339):823–824, 1997. doi: 10.1126/science.278.5339.823.
- J. J. Corbett, P. S. Fischbeck, and S. N. Pandis. Global nitrogen and sulfur inventories for oceangoing ships. *Journal of Geophysical Research: Atmospheres*, 104(D3):3457–3470, 1999.
- J.J. Corbett and H.W. Koehler. Considering alternative input parameters in an activity-based ship fuel consumption and emissions model: Reply to comment by Øyvind Endresen et al. on "updated emissions from ocean shipping". *Journal of Geophysical Research D: Atmospheres*, 109(23):1–8, 2004.
- K. L. Demerjian. A review of national monitoring networks in north america. *Atmospheric Environment*, 34(12–14):1861 – 1884, 2000. ISSN 1352-2310. doi: [http://dx.doi.org/10.1016/S1352-2310\(99\)00452-5](http://dx.doi.org/10.1016/S1352-2310(99)00452-5). URL <http://www.sciencedirect.com/science/article/pii/S1352231099004525>.
- J.-M. Diesch, F. Drewnick, T. Klimach, and S. Borrmann. Investigation of gaseous and particulate emissions from various marine vessel types measured on the banks of the elbe in northern germany. *Atmospheric Chemistry and Physics*, 13(7):3603–3618, 2013.
- G. M. B. Dobson and D. N. Harrison. Measurements of the amount of ozone in the earth's atmosphere and its relation to other geophysical conditions. *Proceedings of the Royal Society of London A: Mathematical, Physical and Engineering Sciences*, 110(756):660–693, 1926. ISSN 0950-1207. doi: 10.1098/rspa.1926.0040.
- EN 14211. *European Standard: EN 14211:2012: Ambient air. Standard method for the measurement of the concentration of nitrogen dioxide and nitrogen monoxide by chemiluminescence*. September 2012.
- Ø. Endresen, E. Sørgård, J.K. Sundet, S.B. Dalsøren, I.S.A. Isaksen, T.F. Berglen, and G. Gravir. Emission from international sea transportation and environmental impact. *Journal of Geophysical Research D: Atmospheres*, 108(17):ACH 14–1 ACH 14–22, 2003.
- Ø. Endresen, E. Sørgård, H.L. Behrens, P.O. Brett, and I.S.A. Isaksen. A historical reconstruction of ships' fuel consumption and emissions. *Journal of Geophysical Research: Atmospheres*, 112(12), 2007.
- V. Eyring, H. W. Köhler, A. Lauer, and B. Lempert. Emissions from international shipping: 2. impact of future technologies on scenarios until 2050. *Journal of Geophysical Research D: Atmospheres*, 110(17):183–200, 2005a.
- V. Eyring, H. W. Köhler, J. Van Aardenne, and A. Lauer. Emissions from international shipping: 1. the last 50 years. *Journal of Geophysical Research D: Atmospheres*, 110(17):171–182, 2005b.
- C. Fayt and M. Van Roozendael. *WinDOAS 2.1*. BIRA-IASB, Uccle, Belgium, 2001.

- B. J. Finlayson-Pitts and J. N. Pitts. *Chemistry of the upper and lower atmosphere : theory, experiments, and applications*. Academic, cop., San Diego, Calif., 2000. ISBN 012257060X 9780122570605.
- N. A. Fuchs. On the stationary charge distribution on aerosol particles in a bipolar ionic atmosphere. *Geofisica Pura e Applicata*, 56(1):185–193, 1963.
- S. V. Hering, M. R. Stolzenburg, F. R. Quant, D. R. O’Berreit, and P. B. Keady. A laminar-flow, water-based condensation particle counter (WCPC). *Aerosol Science and Technology*, 39(7):659–672, 2005.
- W. C. Hinds. *Aerosol technology : properties, behavior, and measurement of airborne particles*. Wiley, New York, 1999. ISBN 0471194107 9780471194101.
- B. J. Huebert, S. G. Howell, D. Covert, T. Bertram, A. Clarke, J. R. Anderson, B. G. Lafleur, W. R. Seebaugh, J. C. Wilson, D. Gesler, B. Blomquist, and J. Fox. Pelti: Measuring the passing efficiency of an airborne low turbulence aerosol inlet. *Aerosol Science and Technology*, 38(8):803–826, 2004.
- IHS Global. IHS Maritime. *Chemin de la Mairie, Perly, Geneva, Switzerland*, 2014.
- P. Intra and N. Tippayawong. An overview of differential mobility analyzers for size classification of nanometer-sized aerosol particles. *Songklanakarin Journal of Science and Technology*, 30(2):243–256, 2008.
- J. P. Jalkanen, A. Brink, J. Kalli, H. Pettersson, J. Kukkonen, and T. Stipa. A modelling system for the exhaust emissions of marine traffic and its application in the baltic sea area. *Atmospheric Chemistry and Physics*, 9(23):9209–9223, 2009. ISSN 16807316 (ISSN).
- J. P. Jalkanen, L. Johansson, J. Kukkonen, A. Brink, J. Kalli, and T. Stipa. Extension of an assessment model of ship traffic exhaust emissions for particulate matter and carbon monoxide. *Atmospheric Chemistry and Physics*, 12(5):2641–2659, 2012. ISSN 16807316 (ISSN).
- J. T. Jayne, D. C. Leard, X. Zhang, P. Davidovits, K. A. Smith, C. E. Kolb, and D. R. Worsnop. Development of an aerosol mass spectrometer for size and composition analysis of submicron particles. *Aerosol Science and Technology*, 33(1-2):49–70, 2000.
- C.-H. Jeong and G. J. Evans. Inter-comparison of a fast mobility particle sizer and a scanning mobility particle sizer incorporating an ultrafine water-based condensation particle counter. *Aerosol Science and Technology*, 43:346–373, 2009. ISSN 0278-6826. doi: 10.1080/02786820802662939.
- J. K. E. Johansson, J. Mellqvist, J. Samuelsson, B. Offerle, J. Moldanova, B. Rappenglück, B. Lefer, and J. Flynn. Quantitative measurements and modeling of industrial formaldehyde emissions in the greater houston area during campaigns in 2009 and 2011. *Journal of Geophysical Research: Atmospheres*, 119(7):4303–4322,

2014. ISSN 2169-8996. doi: 10.1002/2013JD020159. URL <http://dx.doi.org/10.1002/2013JD020159>.
- M. Johansson, B. Galle, T. Yu, L. Tang, D. Chen, H. Li, J. X. Li, and Y. Zhang. Quantification of total emission of air pollutants from beijing using mobile minidoas. *Atmospheric Environment*, 42(29):6926–6933, 2008.
- T. Johnson, R. Caldw, A. Pöcher, A. Mirme, and D. Kittelson. A new electrical mobility particle sizer spectrometer for engine exhaust particle measurements, 2004.
- J. Kalli, T. Karvonen, and T. Makkonen. Sulphur content in ships bunker fuel in 2015: A study on the impacts of the new imo regulations on transportation costs. Report, Publications of the Ministry of Transport and Communication, 2009.
- H. Kaminski, T. A. J. Kuhlbusch, S. Rath, U. Götz, M. Sprenger, D. Wels, J. Polloczek, V. Bachmann, N. Dziurawitz, H.-J. Kiesling, A. Schwiengelshohn, C. Monz, D. Dahmann, and C. Asbach. Comparability of mobility particle sizers and diffusion chargers. *Journal of Aerosol Science*, 57:156–178, 2013.
- J. Kleffmann, G. V. Tapia, I. Bejan, R. Kurtenbach, and P. Wiesen. NO₂ measurement techniques: Pitfalls and new developments. In Ian Barnes and Krzysztof J. Rudziński, editors, *Disposal of Dangerous Chemicals in Urban Areas and Mega Cities*, NATO Science for Peace and Security Series C: Environmental Security, pages 15–28. Springer Netherlands, 2013. ISBN 978-94-007-5033-3. doi: 10.1007/978-94-007-5034-0_2. URL http://dx.doi.org/10.1007/978-94-007-5034-0_2.
- D. Kley and M. McFarland. Chemiluminescence detector for NO and NO₂. *Atmos. Technol.*, 12:63–69, 1980.
- S. G. Kraus. *DOASIS: A Framework Design for DOAS*. PhD thesis, Universität Mannheim, Germany, 2006.
- D. A. Lack, C. D. Cappa, J. Langridge, R. Bahreini, G. Buffaloe, C. Brock, K. Cerully, D. Coffman, K. Hayden, J. Holloway, B. Lerner, P. Massoli, S. M. Li, R. McLaren, A. M. Middlebrook, R. Moore, A. Nenes, I. Nuaaman, T. B. Onasch, J. Peischl, A. Perring, P. K. Quinn, T. Ryerson, J. P. Schwartz, R. Spackman, S. C. Wofsy, D. Worsnop, B. Xiang, and E. Williams. Impact of fuel quality regulation and speed reductions on shipping emissions: implications for climate and air quality. *Environ Sci Technol*, 45(20):9052–60, 2011. ISSN 1520-5851 (Electronic) 0013-936X (Linking). doi: 10.1021/es2013424. URL <http://www.ncbi.nlm.nih.gov/pubmed/21910443>.
- D.A. Lack, J.J. Corbett, T. Onasch, B. Lerner, P. Massoli, P.K. Quinn, T.S. Bates, D.S. Covert, D. Coffman, B. Sierau, S. Herndon, J. Allan, T. Baynard, E. Lovejoy, A.R. Ravishankara, and E. Williams. Particulate emissions from commercial shipping: Chemical, physical, and optical properties. *Journal of Geophysical Research: Atmospheres*, 114(4), 2009.

- B. Y. H. Liu and D. Y. H. Pui. A submicron aerosol standard and the primary, absolute calibration of the condensation nuclei counter. *Journal of Colloid And Interface Science*, 47(1):155–171, 1974.
- W. T. Luke. Evaluation of a commercial pulsed fluorescence detector for the measurement of low-level SO₂ concentrations during the gas-phase sulfur intercomparison experiment. *Journal of Geophysical Research D: Atmospheres*, 102(13):16255–16265, 1997. ISSN 01480227 (ISSN).
- J. Lyyräinen, J. Jokiniemi, and E. Kauppinen. The effect of mg-based additive on aerosol characteristics in medium-speed diesel engines operating with residual fuel oils. *Journal of Aerosol Science*, 33(7):967 – 981, 2002. ISSN 0021-8502. doi: [http://dx.doi.org/10.1016/S0021-8502\(02\)00050-2](http://dx.doi.org/10.1016/S0021-8502(02)00050-2).
- C. S. McNaughton, A. D. Clarke, S. G. Howell, M. Pinkerton, B. Anderson, L. Thornhill, C. Hudgins, E. Winstead, J. E. Dibb, E. Scheuer, and H. Maring. Results from the DC-8 inlet characterization experiment (DICE): Airborne versus surface sampling of mineral dust and sea salt aerosols. *Aerosol Science and Technology*, 41(2):136–159, 2007.
- J. Mellqvist and N. Berg. Final report to vinnova: Identification of gross polluting ships, rg report no. 4, issn 1653 333x. Report, Chalmers University of Technology, 2010.
- J. Mellqvist, N. Berg, and D. Ohlsson. Remote surveillance of the sulfur content and NO_x emissions of ships. In *Second international conference on Harbors, Air Quality and Climate Change (HAQCC)*, Rotterdam, The Netherlands, May 2008.
- J. Mellqvist, J. Ekholm, K. Salo, and J. Beecken. Final report to vinnova: Identification of gross polluting ships to promote a level playing field within the shipping sector, dnr: 2008-03884. Report, Chalmers University of Technology, 2014.
- MEPC. Marine Environment Protection Committee: Interim guidelines for voluntary ship CO₂ emission indexing for use in trials. *IMO, London, United Kingdom*, 2005.
- MEPC. Marine Environment Protection Committee: Amendments to the technical code on control of emission of nitrogen oxides from marine diesel engines - NO_x technical code. *IMO, London, United Kingdom*, 2008.
- A. Michaelowa and K. Krause. International maritime transport and climate policy. *Intereconomics*, 35(3):127–136, 2000. ISSN 0020-5346. doi: 10.1007/BF02927198. URL <http://dx.doi.org/10.1007/BF02927198>.
- J. Moldanova, E. Fridell, O. Popovicheva, B. Demirdjian, V. Tishkova, A. Faccinnetto, and C. Focsa. Characterisation of particulate matter and gaseous emissions from a large ship diesel engine. *Atmospheric Environment*, 43(16):2632–2641, 2009. ISSN 1352-2310. doi: DOI10.1016/j.atmosenv.2009.02.008.

- J. Moldanova, E. Fridell, H. Winnes, S. Holmin-Fridell, J. Boman, A. Jedynska, V. Tishkova, B. Demirdjian, S. Joulie, H. Bladt, N. P. Ivleva, and R. Niessner. Physical and chemical characterisation of PM emissions from two ships operating in European emission control areas. *Atmos. Meas. Tech.*, 6(12):3577–3596, 2013. ISSN 1867-8548. doi: 10.5194/amt-6-3577-2013. URL <http://www.atmos-meas-tech.net/6/3577/2013/>.
- S. Murphy, H. Agrawal, A. Sorooshian, L. T. Padró, H. Gates, S. Hersey, W. A. Welch, H. Jung, J. W. Miller, D. R. Cocker III, A. Nenes, H. H. Jonsson, R. C. Flagan, and J. H. Seinfeld. Comprehensive simultaneous shipboard and airborne characterization of exhaust from a modern container ship at sea. *Environmental Science & Technology*, 43(13):4626–4640, 2009. ISSN 0013936X (ISSN).
- A. O’Keefe and D. A. G. Deacon. Cavity ring-down optical spectrometer for absorption measurements using pulsed laser sources. *Review of Scientific Instruments*, 59(12):2544–2551, 1988. ISSN 00346748 (ISSN).
- D. A. Orsini, Y. Ma, A. Sullivan, B. Sierau, K. Baumann, and R. J. Weber. Refinements to the particle-into-liquid sampler (PILS) for ground and airborne measurements of water soluble aerosol composition. *Atmospheric Environment*, 37(9-10):1243–1259, 2003.
- A. Petzold, J. Hasselbach, P. Lauer, R. Baumann, K. Franke, C. Gurk, H. Schlager, and E. Weingartner. Experimental studies on particle emissions from cruising ship, their characteristic properties, transformation and atmospheric lifetime in the marine boundary layer. *Atmospheric Chemistry and Physics*, 8(9):2387–2403, 2008. ISSN 16807316 (ISSN).
- A. Petzold, E. Weingartner, J. Hasselbach, P. Lauer, C. Kurok, and F. Fleischer. Physical properties, chemical composition, and cloud forming potential of particulate emissions from a marine diesel engine at various load conditions. *Environmental Science and Technology*, 44(10):3800–3805, 2010.
- L. Pirjola, A. Pajunoja, J. Walden, J. P. Jalkanen, T. Rönkkö, A. Kousa, and T. Koskentalo. Mobile measurements of ship emissions in two harbour areas in Finland. *Atmos. Meas. Tech.*, 7(1):149–161, 2014. ISSN 1867-8548. doi: 10.5194/amt-7-149-2014. URL <http://www.atmos-meas-tech.net/7/149/2014/>.
- U. Platt and D. Perner. Measurements of atmospheric trace gases by long path differential uv/visible absorption spectroscopy. *Springer Series in Optical Sciences*, 39:97–105, 1983.
- U. Platt and J. Stutz. *Differential Optical Absorption Spectroscopy - Principles and Applications*. Springer, Berlin, Heidelberg, 2008. ISBN 9783540211938 9783540757764. doi: 10.1007/978-3-540-75776-4.
- A.J. Prata. Measuring SO₂ ship emissions with an ultraviolet imaging camera. *Atmospheric Measurement Techniques*, 7(5):1213–1229, 2014.

- C. Rivera, G. Sosa, H. Wöhrnschimmel, B. De Foy, M. Johansson, and B. Galle. Tula industrial complex (Mexico) emissions of SO₂ and NO₂ during the MCMA 2006 field campaign using a mobile mini-DOAS system. *Atmospheric Chemistry and Physics*, 9(17):6351–6361, 2009.
- H. Schlager, R. Baumann, M. Lichtenstern, A. Petzold, F. Arnold, M. Speidel, C. Gurk, and H. Fischer. Aircraft-based trace gas measurements in a primary European ship corridor. *TAC-Conference*, pages pp. 83–88, 2006. ISSN 92-79-04583-0.
- A. Sorooshian, F. J. Brechtel, Y. Ma, R. J. Weber, A. Corless, R. C. Flagan, and J. H. Seinfeld. Modeling and characterization of a particle-into-liquid sampler (pils). *Aerosol Science and Technology*, 40(6):396–409, 2006. doi: 10.1080/02786820600632282. URL <http://dx.doi.org/10.1080/02786820600632282>.
- UNCTAD. Review of maritime transport 2012, 2012.
- T. Wagner, K. Chance, U. Frieß, M. Gil, F. Goutail, G. Hönninger, P. V. Johnston, K. Karlsen-Tornkvist, I. Kostadinov, H. Leser, A. Petritoli, A. Richter, M. Van Roozendaal, and U. Platt. Correction of the ring effect and IO-effect for DOAS observations of scattered sunlight, 2001.
- R. J. Weber, D. Orsini, Y. Daun, Y.-N. Lee, P. J. Klotz, and F. Brechtel. A particle-into-liquid collector for rapid measurement of aerosol bulk chemical composition. *Aerosol Science and Technology*, 35(3):718–727, 2001.
- J. M. Welles and D. K. McDermitt. *Measuring Carbon Dioxide in the Atmosphere*, pages 287–320. Agronomy Monograph. American Society of Agronomy, Crop Science Society of America, and Soil Science Society of America, 2005. doi: 10.2134/agronmonogr47.c13. URL <https://dl.sciencesocieties.org/publications/books/abstracts/agronomymonogra/micrometeorolog/287>.
- A. Wiedensohler. An approximation of the bipolar charge distribution for particles in the submicron size range. *Journal of Aerosol Science*, 19(3):387–389, 1988.
- E. J. Williams, B. M. Lerner, P. C. Murphy, S. C. Herndon, and M. S. Zahniser. Emissions of NO_x, SO₂, CO, and HCHO from commercial marine shipping during Texas Air Quality Study (TexAQSt) 2006. *Journal of Geophysical Research. D. Atmospheres*, 114:D21306, 2009. ISSN 0148-0227. doi: doi:10.1029/2009JD012094.
- H. Winnes and E. Fridell. Particle emissions from ships: Dependence on fuel type. *Journal of the Air and Waste Management Association*, 59(12):1391–1398, 2009.
- H. Winnes and E. Fridell. Emissions of NO_x and particles from manoeuvring ships. *Transportation Research Part D: Transport and Environment*, 15(4):204–211, 2010. cited By 10.
- N. Zimmerman, C.-H. Jeong, J. M. Wang, M. Ramos, J. S. Wallace, and G. J. Evans. A source-independent empirical correction procedure for the fast mobility and engine exhaust particle sizers. *Atmospheric Environment*, 100(0):178 – 184, 2015. ISSN 1352-2310. doi: <http://dx.doi.org/10.1016/j.atmosenv.2014.10.054>.

